Electronic Supporting Information for:

Isolation and structural characterisation of rhodium(III) η^2–fluoroarene complexes: experimental verification of predicted regioselectivity

Matthew R. Gyton,‡ Amy E. Kynman,‡ Baptiste Leforestier, Angelo Gallo, Józef R. Lewandowski, and Adrian B. Chaplin

Department of Chemistry, University of Warwick, Gibbet Hill Road, Coventry, CV4 7AL.
Email: a.b.chaplin@warwick.ac.uk; ‡ These authors contributed equally.

Table of contents

1. General experimental methods

All manipulations were performed under an atmosphere of argon (N4.8) using Schlenk and glovebox techniques unless otherwise stated. Glassware was oven dried at 150 °C overnight and flame-dried under vacuum prior to use. Molecular sieves were activated by heating at 300 °C *in vacuo* overnight. CD_2Cl_2 was freeze-pump-thaw degassed and dried over 3 Å molecular sieves. C_6H_6 was distilled from sodium and benzophenone and stored over 3 Å molecular sieves Fluoroarenes were pre-dried over Al_2O_3, distilled from calcium hydride and dried over two successive batches of 3 Å molecular sieves. Other anhydrous solvents were purchased from Acros or Sigma-Aldrich, freeze-thaw degassed and stored over 3 Å molecular sieves. $Na[B(3,5\text{-}(CF_3)_2C_6H_3)_4]$[1] CNC-Me·2HBr[2] and $[Rh(biph)Cl(tBu_2PCH_2PtBu_2)]$[3] were prepared following literature procedures. All other reagents are commercially available and were used as supplied. Solution and solid-state NMR spectra were recorded on Bruker spectrometers at 298 K unless otherwise stated. NMR spectra in fluoroarenes were recorded using an internal capillary of C_6D_6 and externally referenced to $SiMe_4$. Chemical shifts are quoted in ppm and coupling constants in Hz. Crystallographic data was collected on a dual source Rigaku Oxford diffraction SuperNova diffractometer. HR ESI-MS were recorded on a Bruker MaXis mass spectrometer and microanalyses performed at the London Metropolitan University by Stephen Boyer. IR spectra were recorded in air on a Bruker Alpha Platinum ATR FT-IR spectrometer at 298 K.

2. Preparation of $[Rh(CNC\text{-}Me)(biph)(\kappa^1\text{–}ClCH_2Cl)][B(3,5\text{-}(CF_3)_2C_6H_3)_4]$ 2

A suspension of Ag_2O (23.5 mg, 101 µmol), CNC-Me·2HBr (40.7 mg, 101 µmol) and $Na[B(3,5\text{-}(CF_3)_2C_6H_3)_4]$ (98.6 mg, 111 µmol) in CH_2Cl_2 (*ca*. 2 mL) was stirred in the dark for 18 h. The solution was filtered, washing the precipitate with additional CH_2Cl_2 (3 x 1 mL) before it was discarded, and volatiles removed *in vacuo*. Solid [Rh(biph)Cl(dtbpm)] (60.9 mg, 102 µmol) and CH_2Cl_2 (*ca*. 2 mL) were added and the resulting solution stirred at RT for 18 h. Volatiles were removed *in vacuo* and the organometallic intermediate extracted into Et_2O (3 x 3 mL) and the solvent removed *in vacuo*. Solid $Na[B(3,5\text{-}(CF_3)_2C_6H_3)_4]$ (99.2 mg, 112 µmol) and CH_2Cl_2 (*ca*. 2 mL) were added and the resulting suspension stirred at room temperature for 18 h. The solution was filtered, washing the precipitate with additional CH_2Cl_2 (3 x 1mL) before it was discarded, and the product obtained as yellow-orange blocks after successive recrystallisation from CH_2Cl_2/hexane at RT. Yield: 117 mg (80%).

^{1}H NMR (500 MHz, CD_2Cl_2): δ 8.33 (t, $^3J_{HH}$ = 8.2, 1H, py), 7.68–7.81 (m, 8H, Ar^F), 7.65 (d, $^3J_{HH}$ = 2.0, 2H, NCH), 7.59 (d, $^3J_{HH}$ = 8.2, 2H, py), 7.56 (br, 4H, Ar^F), 7.54 (br, 2H, biph), 7.00 (vbr, fwhm = 20 Hz, 2H, biph), 6.92 (d, $^3J_{HH}$ = 2.0, 2H, NCH), 6.76 (vbr, fwhm = 60 Hz, 2H, biph), 5.33 (s, 2H, free CH_2Cl_2), 3.21 (s, 6H, CH_3). One of the biph signals is not observed, presumably as a consequence of structural dynamics.

^{13}C{^{1}H} NMR (126 MHz, CD_2Cl_2): δ 182.4 (d, $^1J_{RhC}$ = 44, NCN), 162.3 (q, $^1J_{CB}$ = 50, Ar^F), 151.1 (s, py), 144.9 (s, py), 135.4 (s, Ar^F), 129.3 (qq, $^1J_{FC}$ = 32, $^1J_{CB}$ = 3, Ar^F), 126.5 (biph), 125.6 (s, NCH), 125.1 (q, $^1J_{FC}$ = 272, Ar^F), 123.7 (s, biph),121.4 (s, biph), 118.1 (sept, $^3J_{FC}$ = 4, Ar^F), 118.0 (s, NCH), 108.3 (s, py), 37.9 (s, CH_3). Three biph signals are not observed, presumably as a consequence of structural dynamics.

Anal. Calcd. for $C_{58}H_{35}BCl_2F_{24}N_5Rh$ (1442.53 gmol^{-1}): C, 48.29; H, 2.45; N, 4.86. Found C, 48.40; H, 2.37; N, 4.81.

HR ESI-MS (positive ion, 4 kV): 494.0852 ($[M – CH_2Cl_2]^+$, calcd 494.0847) *m*/*z*.

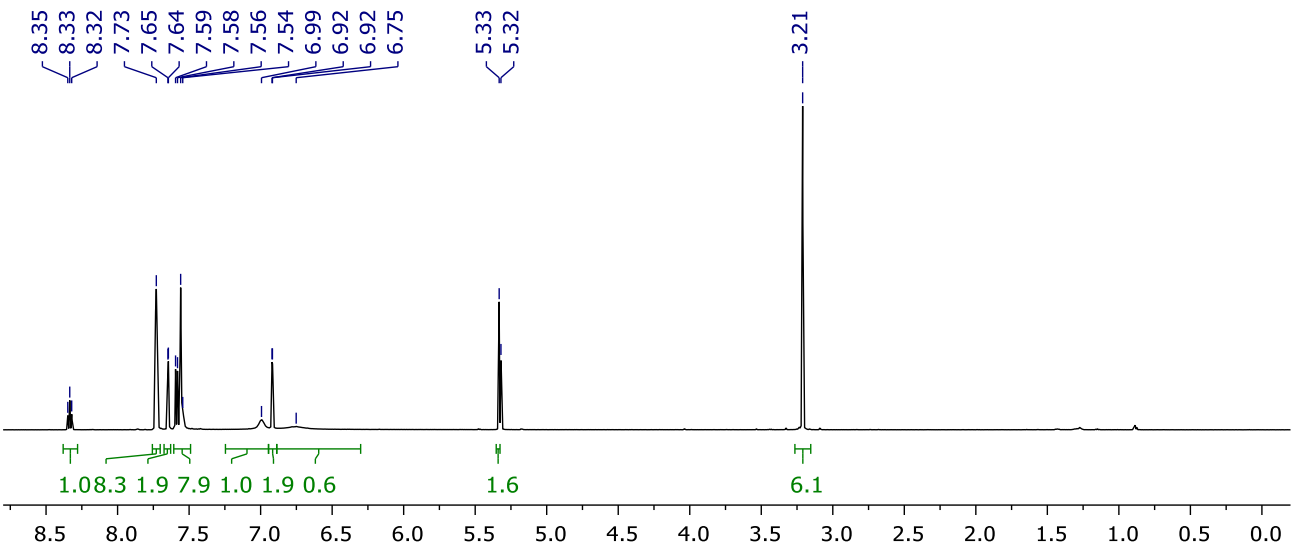

Figure S1. ^{1}H NMR spectrum of **2** (CD_2Cl_2, 600 MHz).

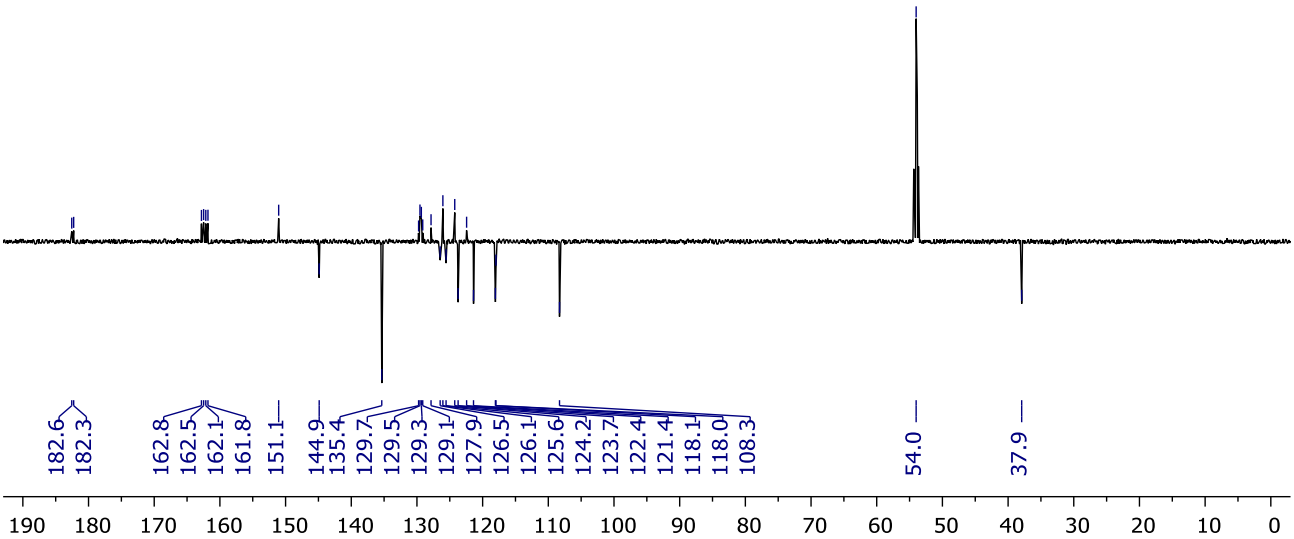

Figure S2. ^{13}C{^{1}H} APT NMR spectrum of **2** (CD_2Cl_2, 151 MHz).

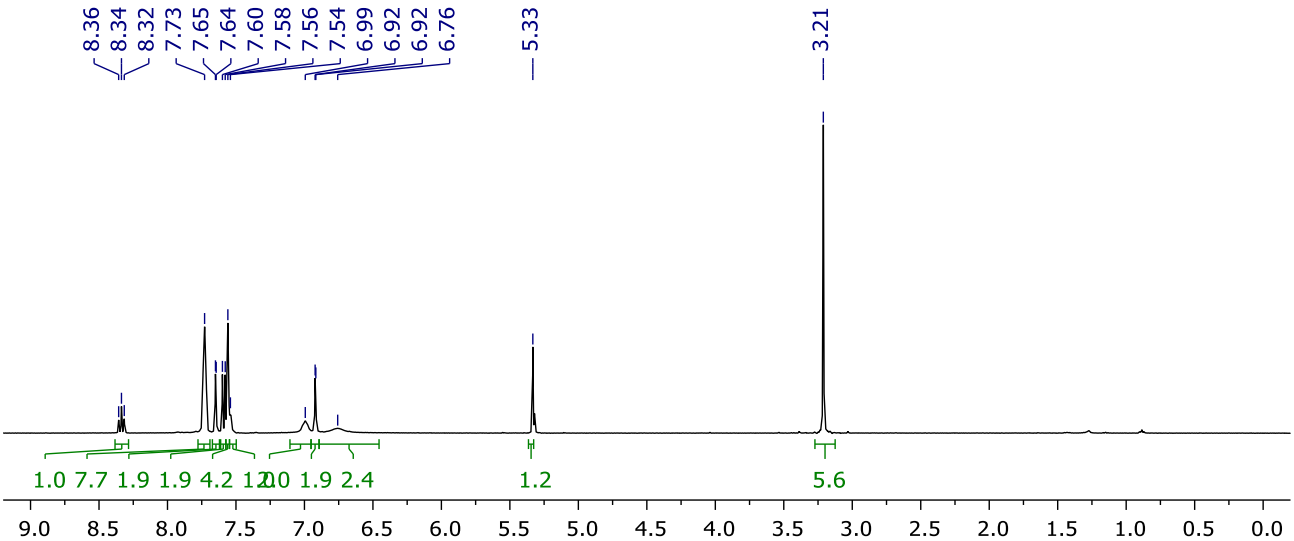

Figure S3. ^{1}H NMR spectrum of **2** (CD_2Cl_2, 400 MHz).

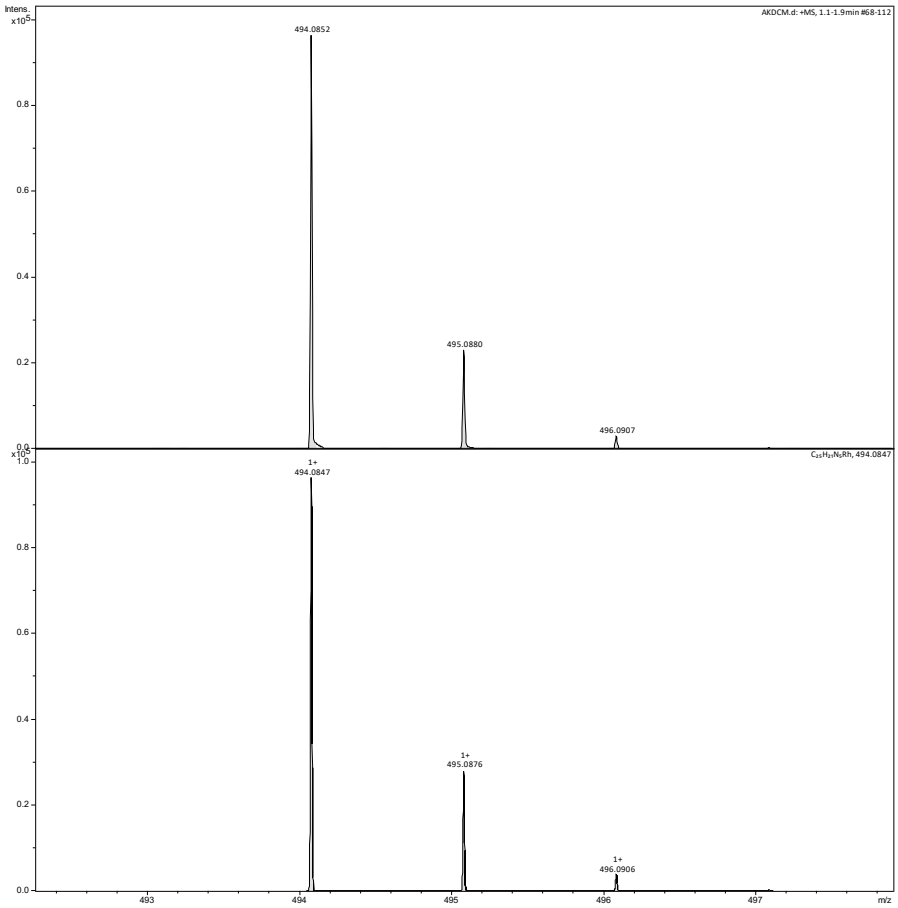

Figure S4. HR ESI-MS of **2**.

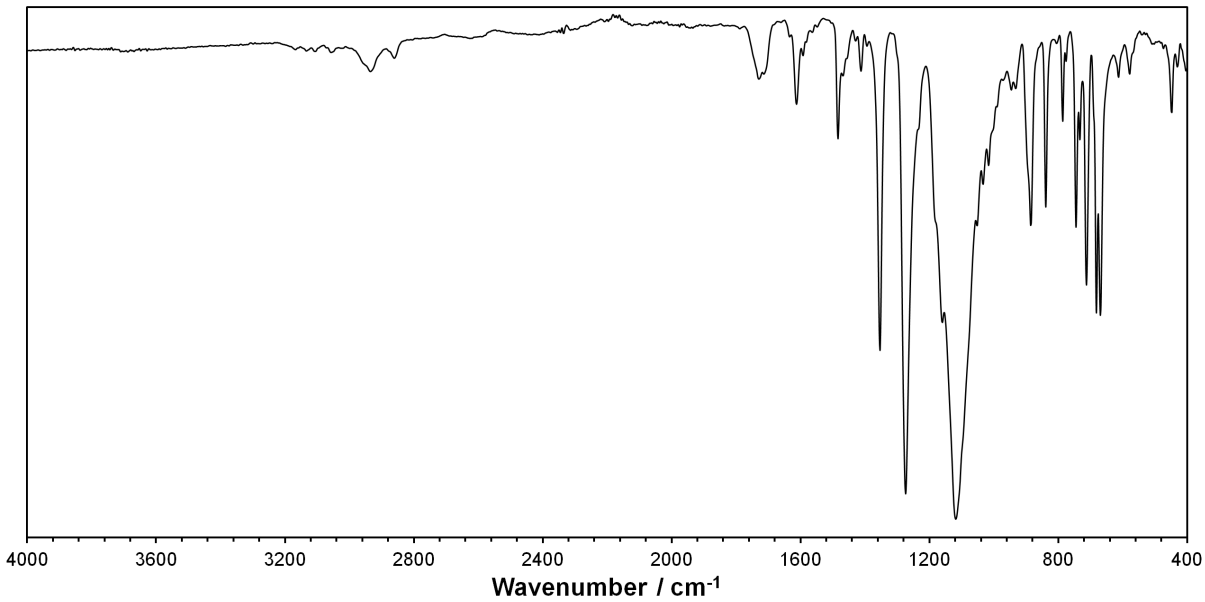

Figure S5. ATR IR spectrum of **2**.

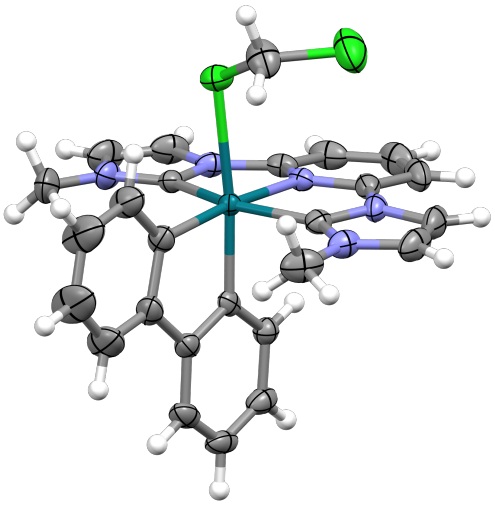

Figure S6. Solid-state structure of **2**. Thermal ellipsoids at 50% probability, minor disordered component (Rh–Cl<u>CH$_2$Cl</u>) and [B(3,5-(CF$_3$)$_2$C$_6$H$_3$)$_4$]$^-$ anion omitted for clarity. Selected bond lengths (Å) and angles (°) associated with dichloromethane coordination: Rh–Cl, 2.5932(7); *trans*-C–Rh–Cl, 174.01(7); *trans*-C-Rh, 2.017(3).

3. Analysis of 2 by VT NMR spectroscopy.

Data were collected using a solution of **2** (14.4 mg, 10.0 μmol) in CD_2Cl_2 (0.5 mL) within a J. Young's valve NMR tube and a 600 MHz Bruker spectrometer. The sample was equilibrated at each temperature for at least 5 min before data acquisition (Figure S7).

The dynamics observed by ^{1}H NMR spectroscopy were modelled using the four biphenyl resonances in the region 7.30 – 6.20 ppm (Table S1, Figure S8). Reference line widths and coupling constants were fixed following analysis of low temperature data (200 – 225 K). Eyring analysis (Figure S9) of the associated rate constants yielded $\Delta H^{\ddagger}$ = 75 ± 1 kJ mol^{-1} and $\Delta S^{\ddagger}$ = +80 ± 5 J K^{-1} mol^{-1}, with $\Delta G^{\ddagger}_{298K}$ = 52 ± 3 kJ mol^{-1}.

Table S1. Variable temperature ^{1}H NMR data for **2**.

T **/ K**	**log(*k*)**	***k*** **/ s^{-1}**	**ln(*k*/*T*)**
240	0.3792	2.39	-4.607
250	1.1533	14.23	-2.866
260	1.7885	61.45	-1.443
268	2.1846	152.97	-0.561
273	2.5425	348.74	0.245
298	3.7652	5823.71	2.973
308	4.1172	13097.85	3.750

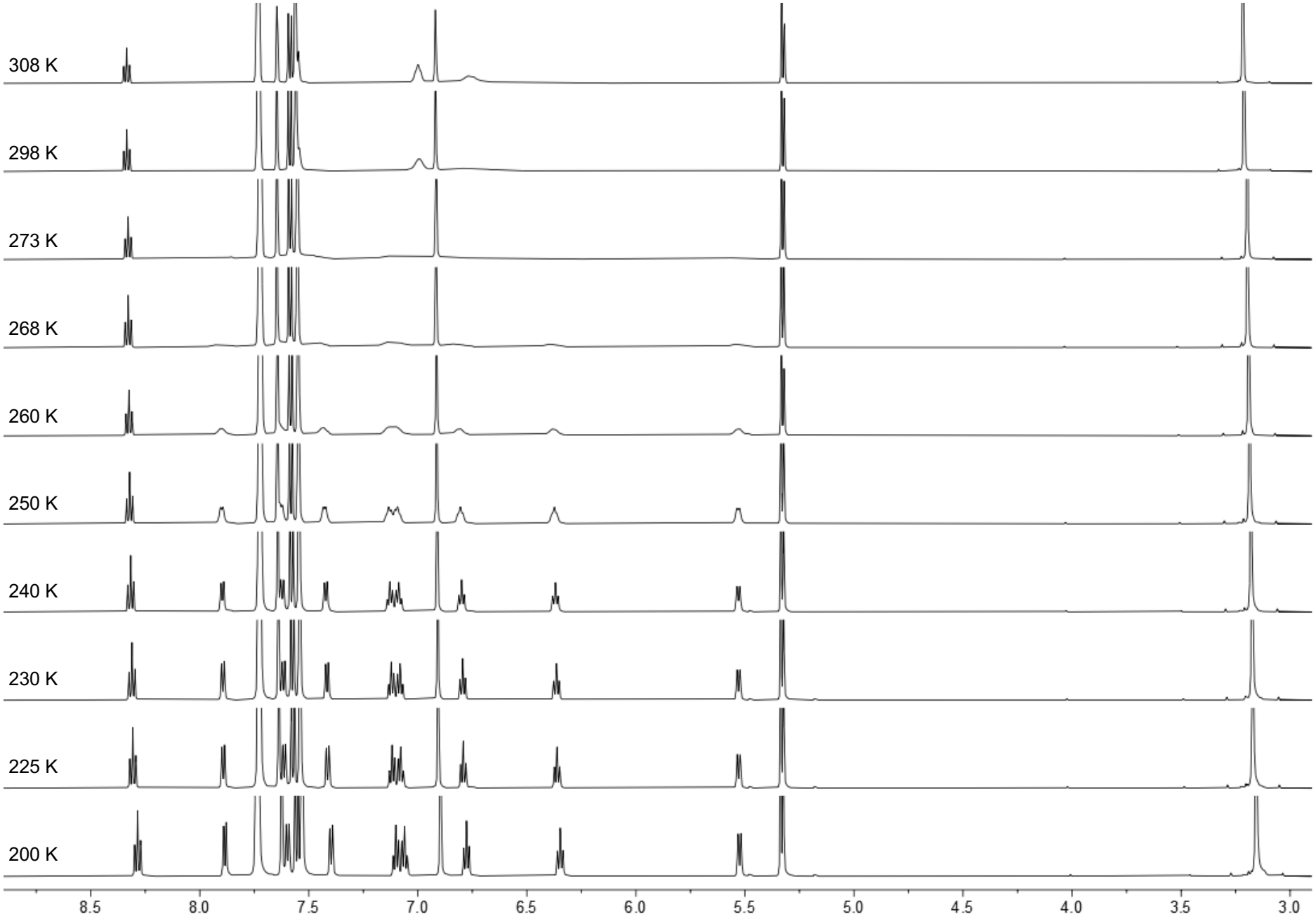

Figure S7. Variable temperature ^{1}H NMR spectra of **2** (CD_2Cl_2, 600 MHz).

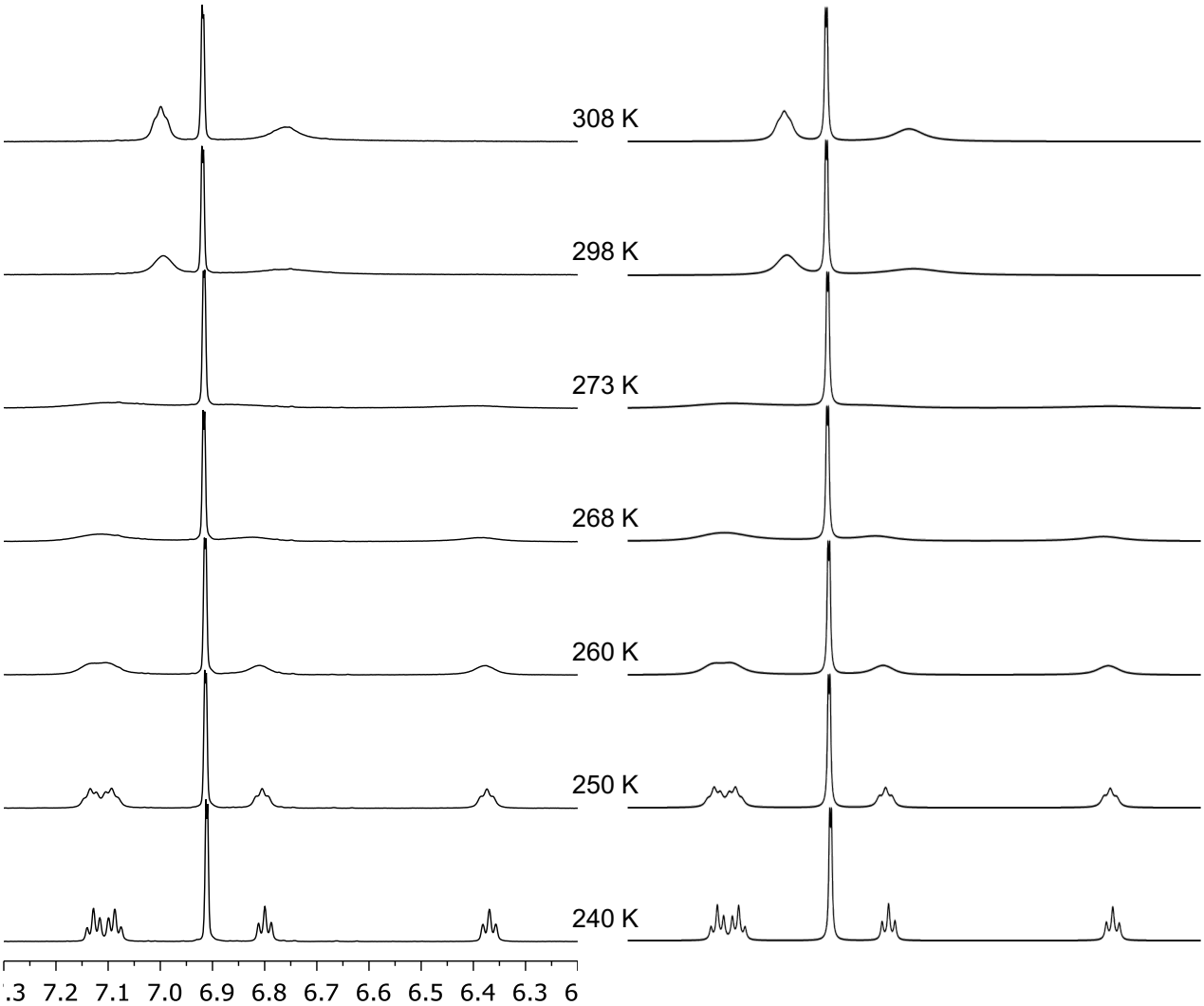

Figure S8. Experimental and simulated ^{1}H NMR spectra of **2** (CD_2Cl_2, 600 MHz).

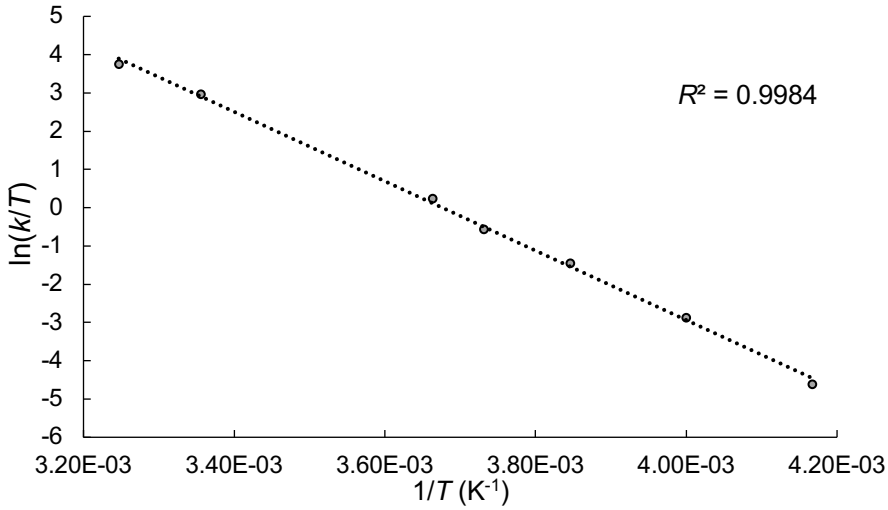

Figure S9. Eyring plot for the dynamics observed in **2**.

4. NMR scale reactions of 2 with fluoroarenes

Complex **2** (14.4 mg, 10.0 μmol) and fluoroarene solvent (0.5 mL) were mixed within a J. Young's valve NMR tube and the resulting solution analysed by ^{1}H and $^{19}F\{^{1}H\}$ NMR spectroscopy.

4.1 Arene = FC_6H_5

Following the general procedure, an orange solution was obtained. Analysis by ^{1}H NMR spectroscopy indicated the liberation of one equivalent of CH_2Cl_2 (δ 4.73) into solution. The $^{19}F\{^{1}H\}$ NMR spectrum showed only signals for the $[B(3,5\text{-}(CF_3)_2C_6H_3)_4]^-$ anion (δ -62.5) and the solvent (δ -113.3).

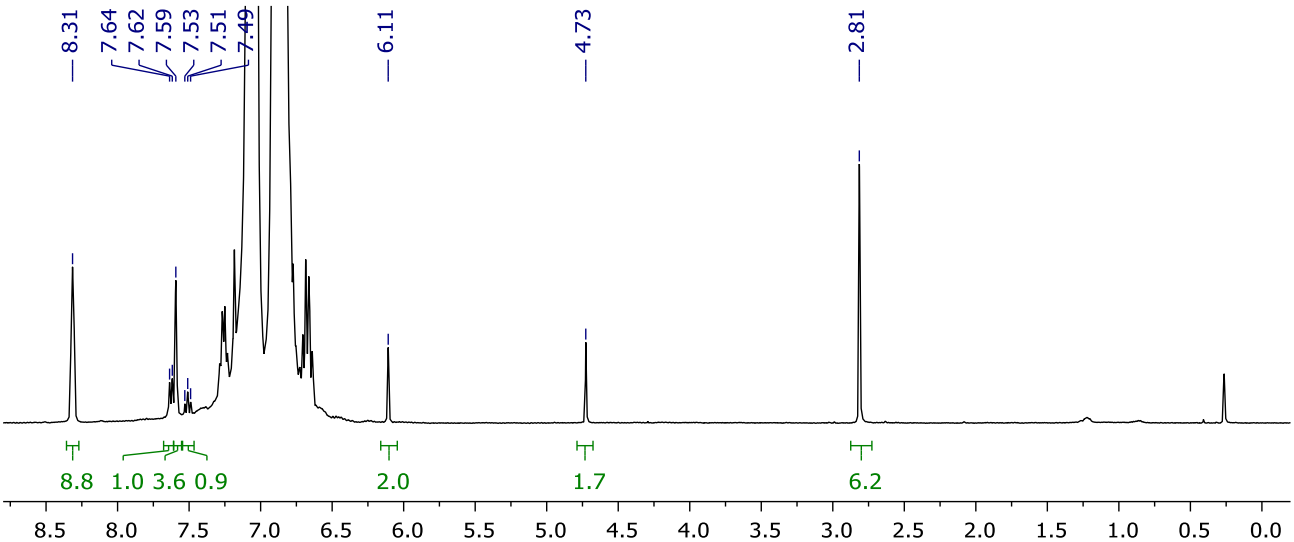

Figure S10. ^{1}H NMR spectrum recorded after **2** was dissolved in FC_6H_5 (400 MHz).

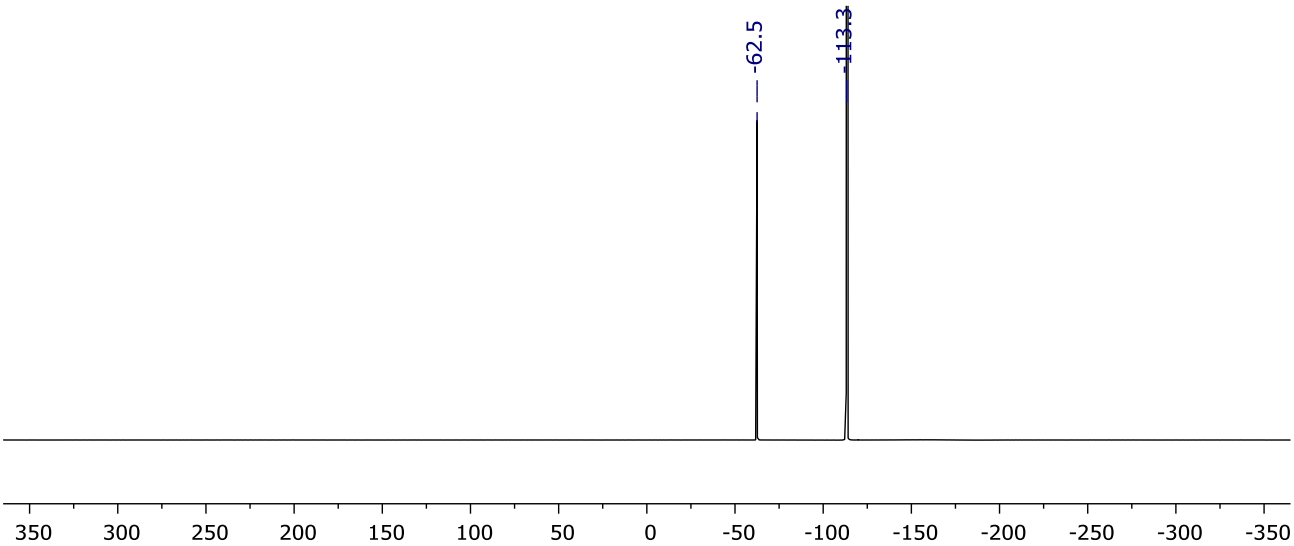

Figure S11. $^{19}F\{^{1}H\}$ NMR spectrum recorded after **2** was dissolved in FC_6H_5 (377 MHz).

4.2 Arene = 1,2-$F_2C_6H_4$

Following the general procedure, an orange solution was obtained. Analysis by ^{1}H NMR spectroscopy indicated the liberation of one equivalent of CH_2Cl_2 (δ 4.91) into solution. The ^{19}F{^{1}H} NMR spectrum showed only signals for the $[B(3,5\text{-}(CF_3)_2C_6H_3)_4]^-$ anion (δ -63.1) and the solvent (δ -139.6).

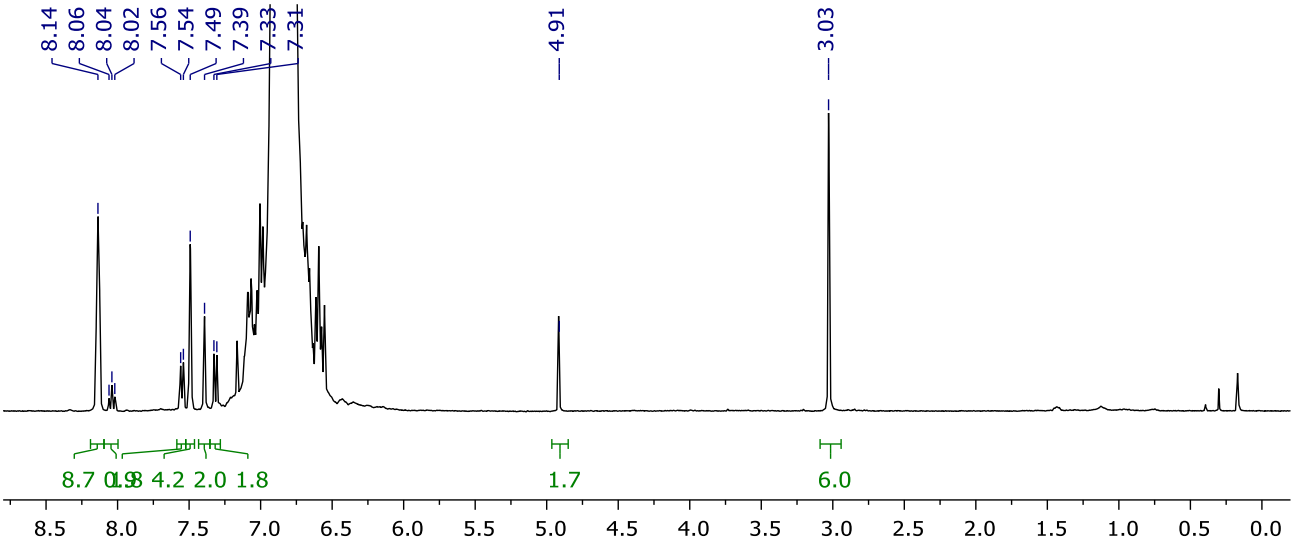

Figure S12. ^{1}H NMR spectrum recorded after **2** was dissolved in 1,2-$F_2C_6H_4$ (400 MHz).

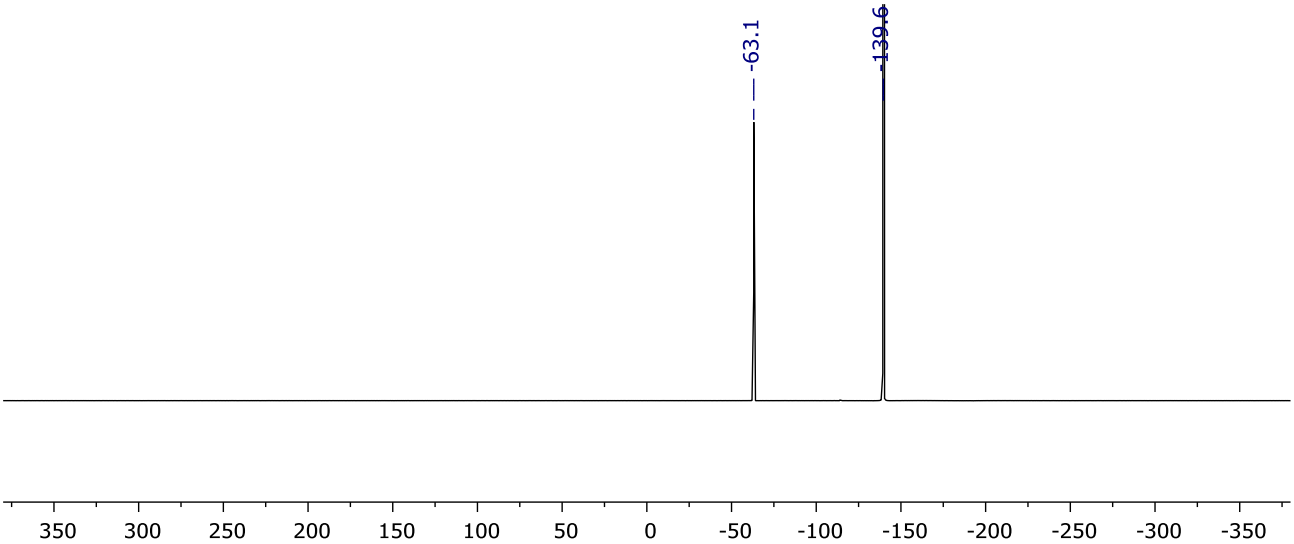

Figure S13. ^{19}F{^{1}H} NMR spectrum recorded after **2** was dissolved in 1,2-$F_2C_6H_4$ (377 MHz).

4.3 Arene = 1,3-$F_2C_6H_4$

Following the general procedure, an orange solution was obtained. Analysis by ^{1}H NMR spectroscopy indicated the liberation of one equivalent of CH_2Cl_2 (δ 5.01) into solution. The ^{19}F{^{1}H} NMR spectrum showed only signals for the $[B(3,5\text{-}(CF_3)_2C_6H_3)_4]^-$ anion (δ -62.9) and the solvent (δ -110.7).

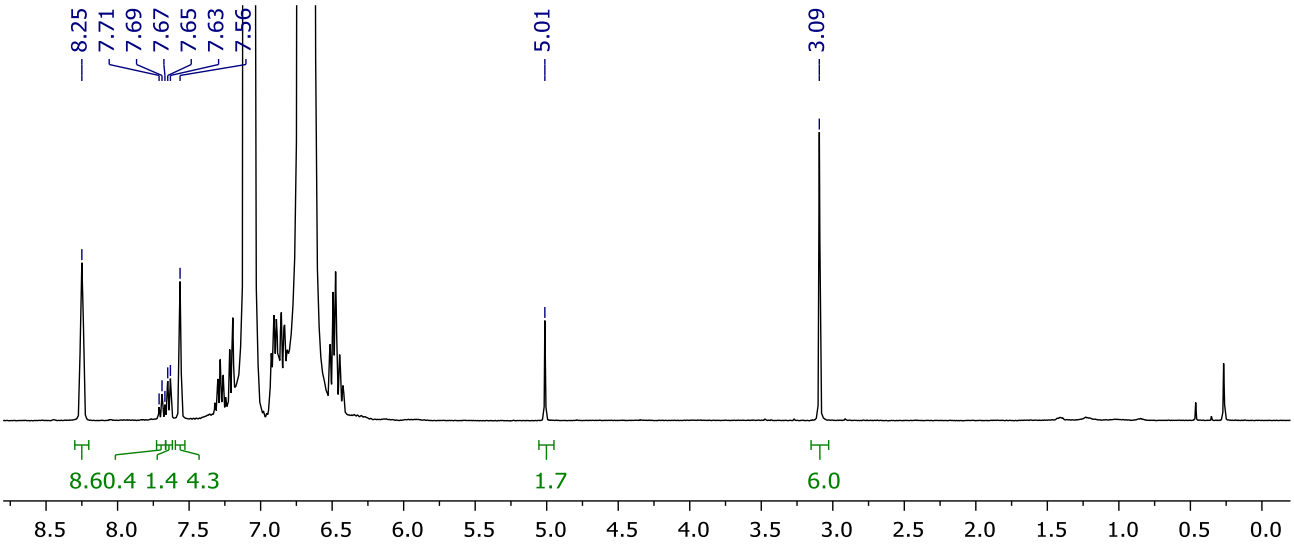

Figure S14. ^{1}H NMR spectrum recorded after **2** was dissolved in 1,3-$F_2C_6H_4$ (400 MHz).

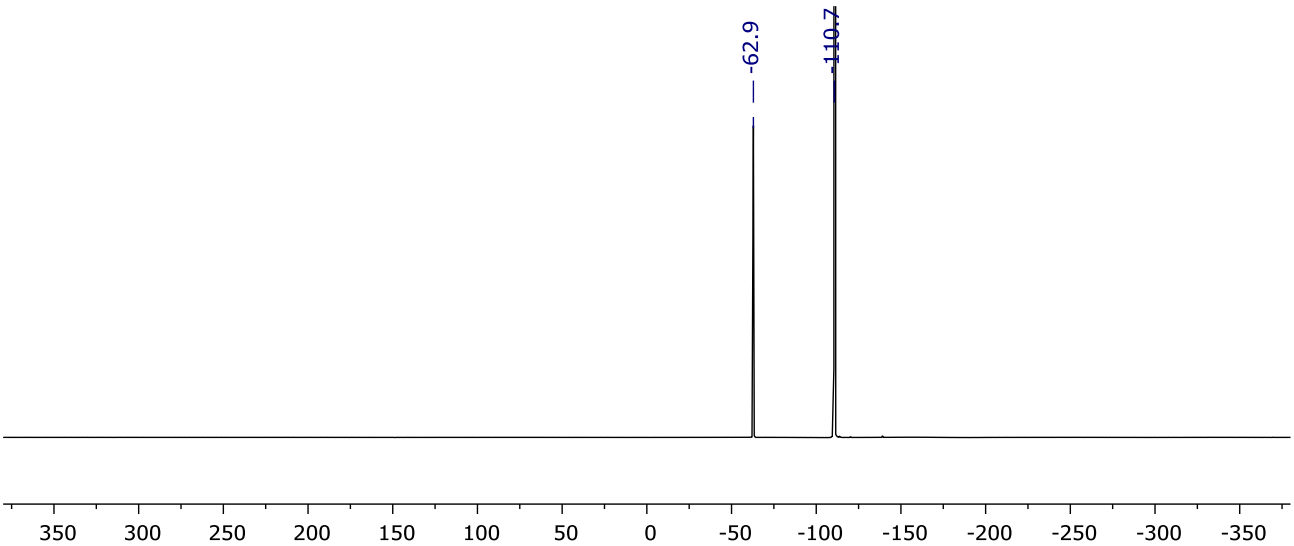

Figure S15. ^{19}F{^{1}H} NMR spectrum recorded after **2** was dissolved in 1,3-$F_2C_6H_4$ (377 MHz).

4.4 Arene = 1,4-$F_2C_6H_4$

Following the general procedure, a suspension was obtained with an orange precipitate. Full dissolution was only obtained with warming. Analysis by ^{1}H NMR spectroscopy at 298 K after initial mixing indicated the liberation of CH_2Cl_2 (*ca.* 10 equivalents per complex, δ 5.06) into solution. The ^{19}F{^{1}H} NMR spectrum showed only signals for the $[B(3,5\text{-}(CF_3)_2C_6H_3)_4]^-$ anion (δ -62.8) and the solvent (δ -120.3). ^{1}H NMR spectra recorded at 351 K and immediately after cooling to 298 K before the onset of crystallisation are consistent with the liberation of one equivalent of CH_2Cl_2 into solution (δ_{351K} 5.00; δ_{298K} 5.05).

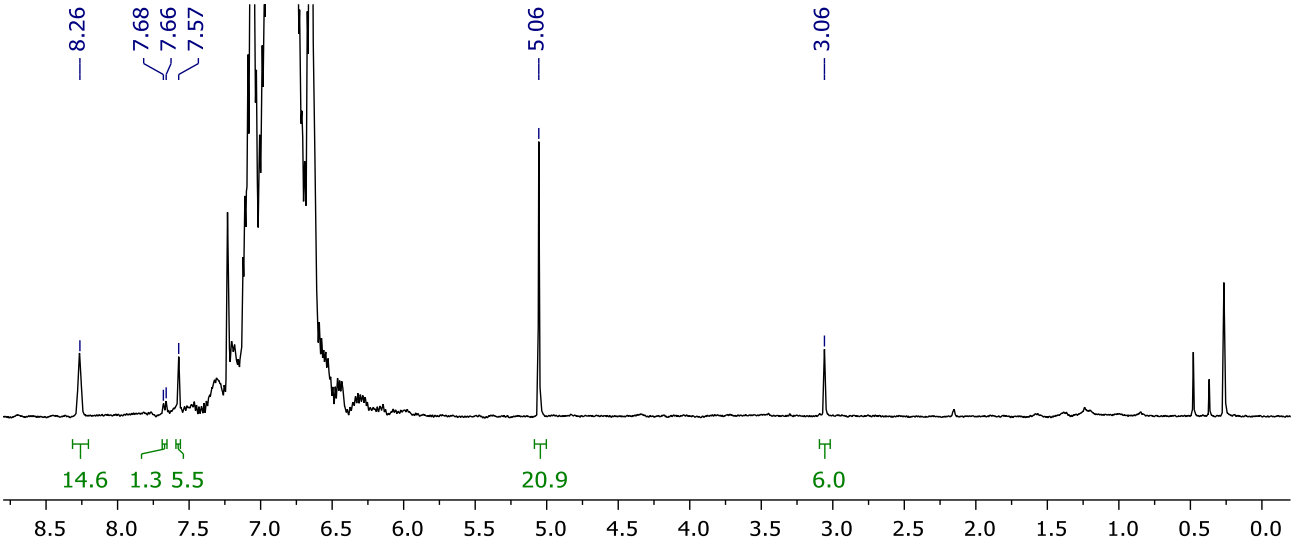

Figure S16. ^{1}H NMR spectrum recorded after **2** was mixed with 1,4-$F_2C_6H_4$ (298 K, 400 MHz).

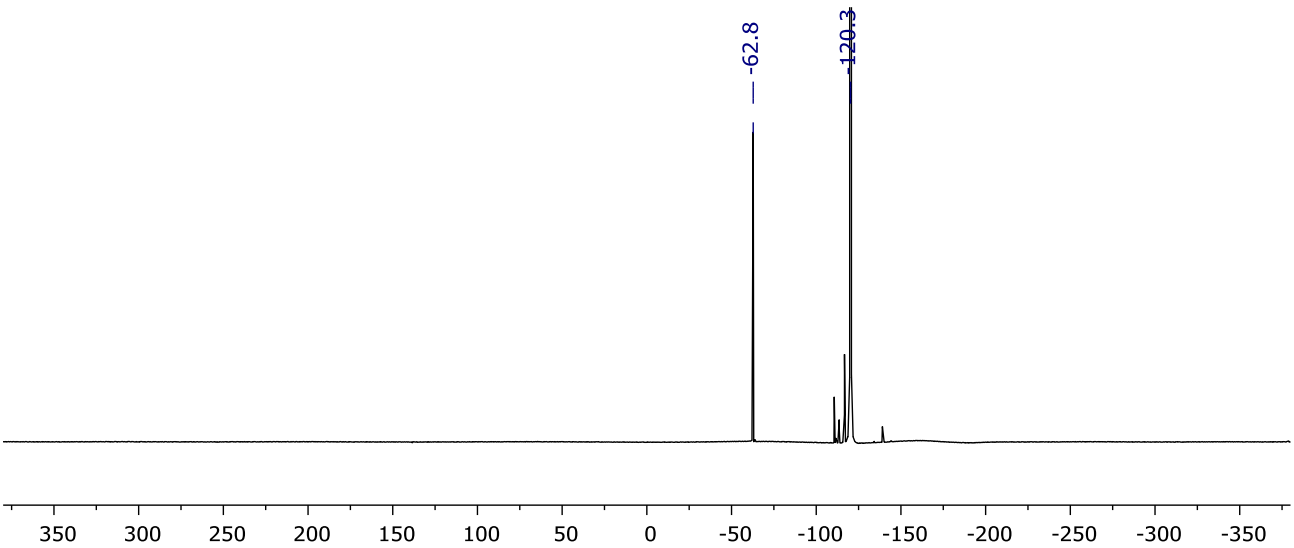

Figure S17. ^{19}F{^{1}H} NMR spectrum recorded after **2** was mixed with 1,4-$F_2C_6H_4$ (298 K, 377 MHz).

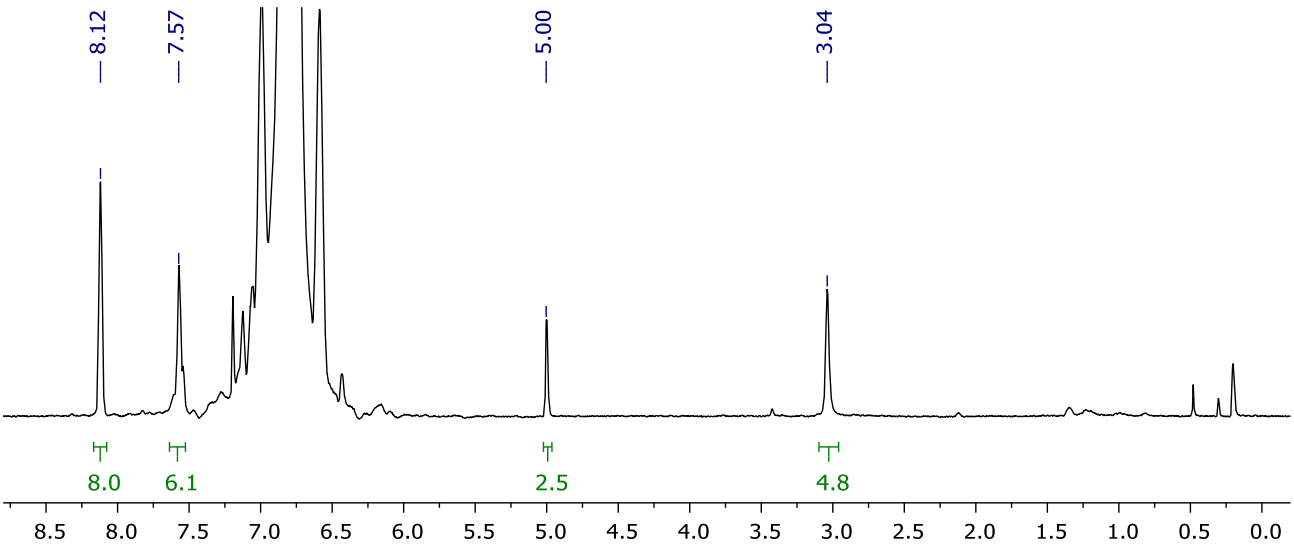

Figure S18. ^{1}H NMR spectrum recorded after **2** was heated until dissolution in 1,4-$F_2C_6H_4$ (351 K, 400 MHz).

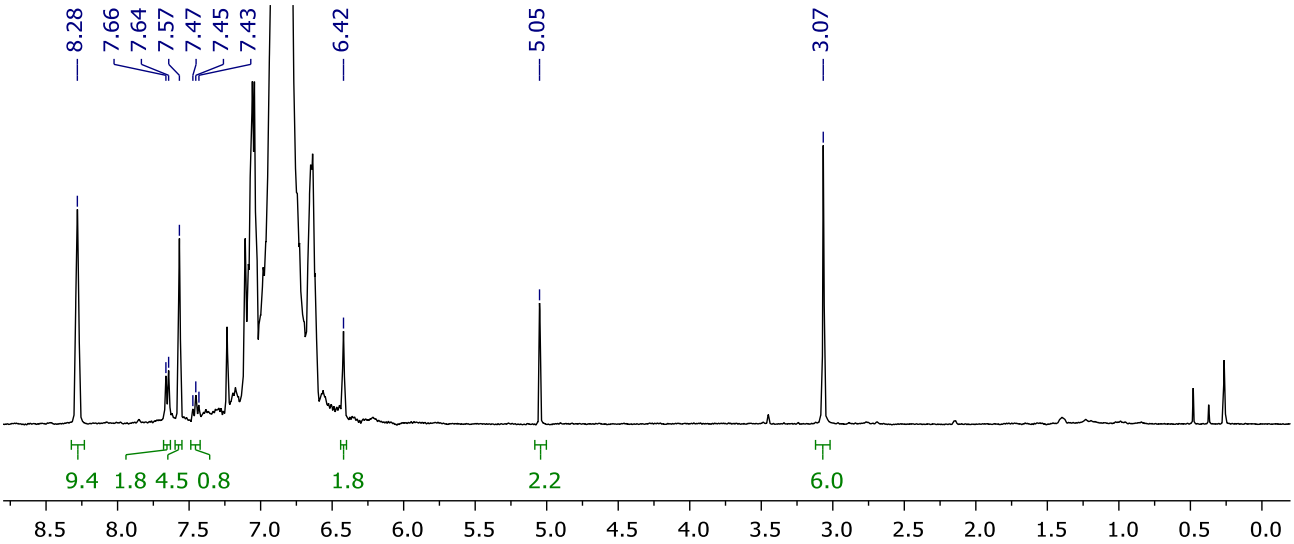

Figure S19. ^{1}H NMR spectrum recorded after **2** was heated until dissolution in 1,4-$F_2C_6H_4$ (298 K, 400 MHz).

5. Preparation of [Rh(CNC-Me)(biph)(η^2-arene)][B(3,5-$(CF_3)_2C_6H_3)_4$] 1

5.1 General procedure

A solution of **2** in the respective fluoroarene (*ca.* 2 mL) was briefly mixed before volatiles were removed *in vacuo*. The product was then recrystallised as orange bocks by layering a solution of the crude product in the respective fluoroarene with hexane and then storage at RT.

5.2 Arene = FC_6H_5 (1b)

Following the general procedure using **2** (40.0 mg, 27.7 µmol) and C_6H_5F afforded **1b**. Yield: 29.3 mg (73%).

No absorbances attributed to bound fluoroarene could be detected on analysis by ATR IR spectroscopy. Analysis of a sample dissolved in CD_2Cl_2 by ^1H and ^{19}F NMR spectroscopy indicated the liberation of one equivalent of FC_6H_5 into solution (δ_{19F} -113.9).

Anal. Calcd. for $C_{63}H_{38}BF_{25}N_5Rh$ (1453.71 gmol^{-1}): C, 52.05; H, 2.63; N, 4.82. Found C, 52.07; H, 2.65; N, 4.76.

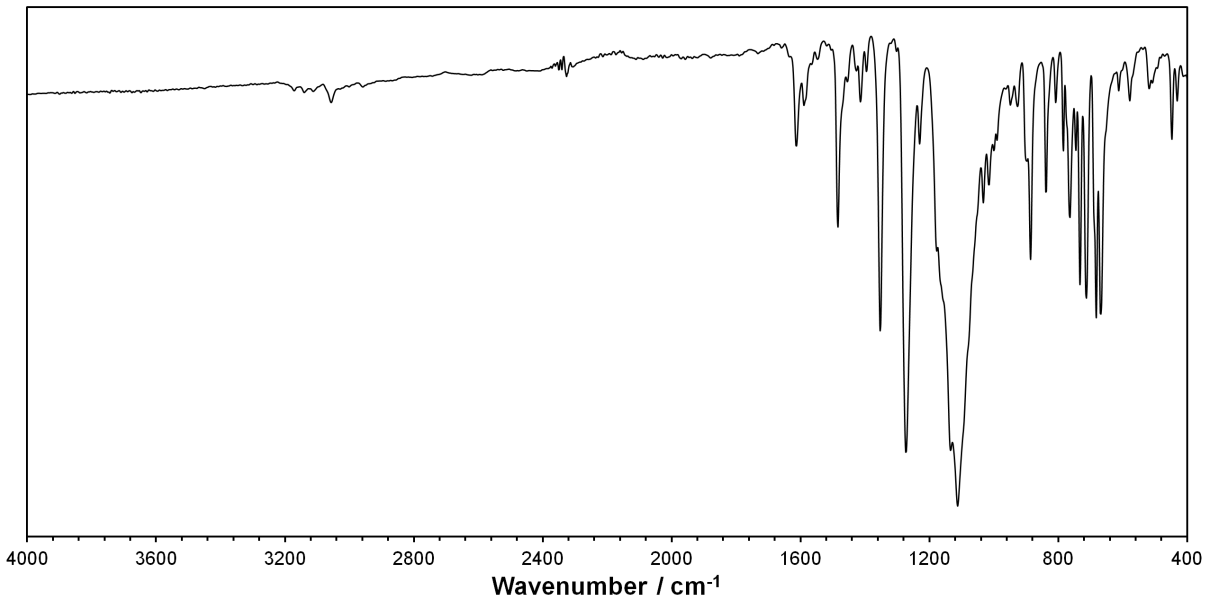

Figure S20. ATR IR spectrum of **1b**.

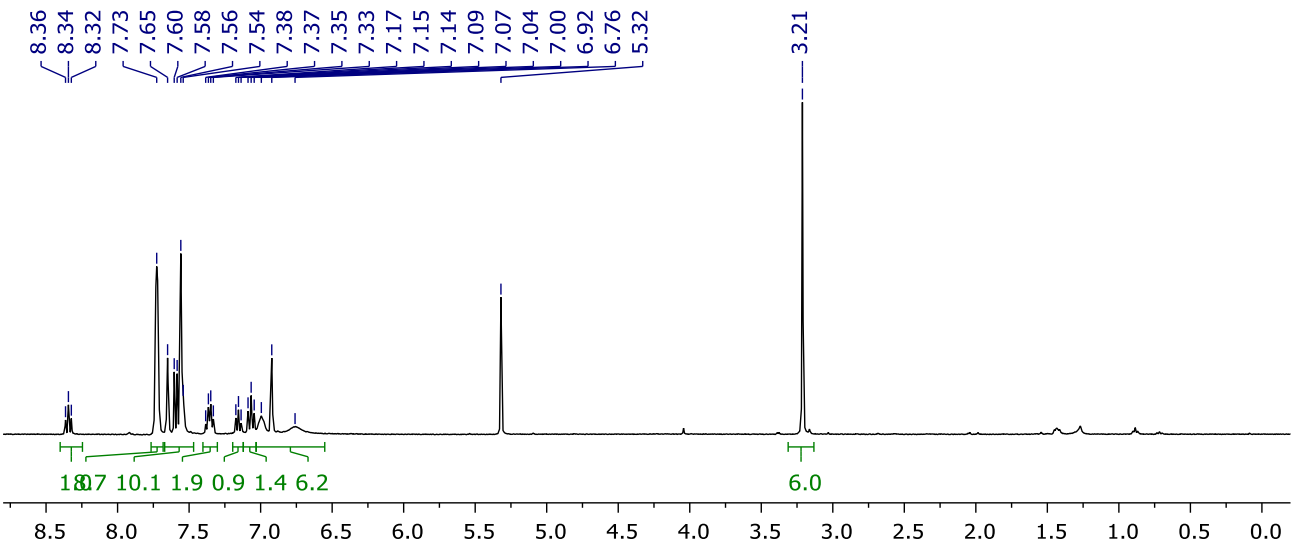

Figure S21. ^{1}H NMR spectrum recorded after **1b** was dissolved in CD_2Cl_2 (400 MHz).

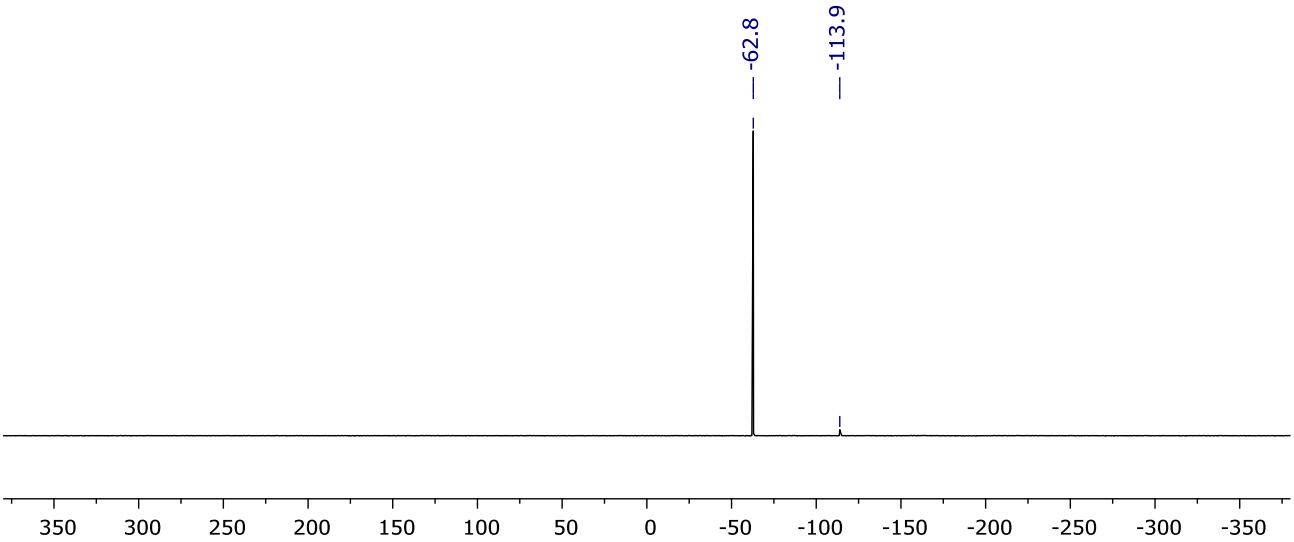

Figure S22. ^{19}F{^{1}H} NMR spectrum recorded after **1b** was dissolved in CD_2Cl_2 (377 MHz).

5.3 Arene = 1,2-$F_2C_6H_4$ (1c)

Following the general procedure using **2** (40.0 mg, 27.7 µmol) and 1,2-$F_2C_6H_4$ afforded **1c**. Yield: 25.0 mg (61%).

No absorbances attributed to bound fluoroarene could be detected on analysis by ATR IR spectroscopy. Analysis of a sample dissolved in CD_2Cl_2 by ^{1}H and ^{19}F NMR spectroscopy indicated the liberation of one equivalent of 1,2-$F_2C_6H_4$ into solution (δ_{19F} -139.4).

Anal. Calcd. for $C_{63}H_{37}BF_{26}N_5Rh$ (1471.70 gmol^{-1}): C, 51.42; H, 2.53; N, 4.76. Found C, 51.44; H, 2.43; N, 4.70.

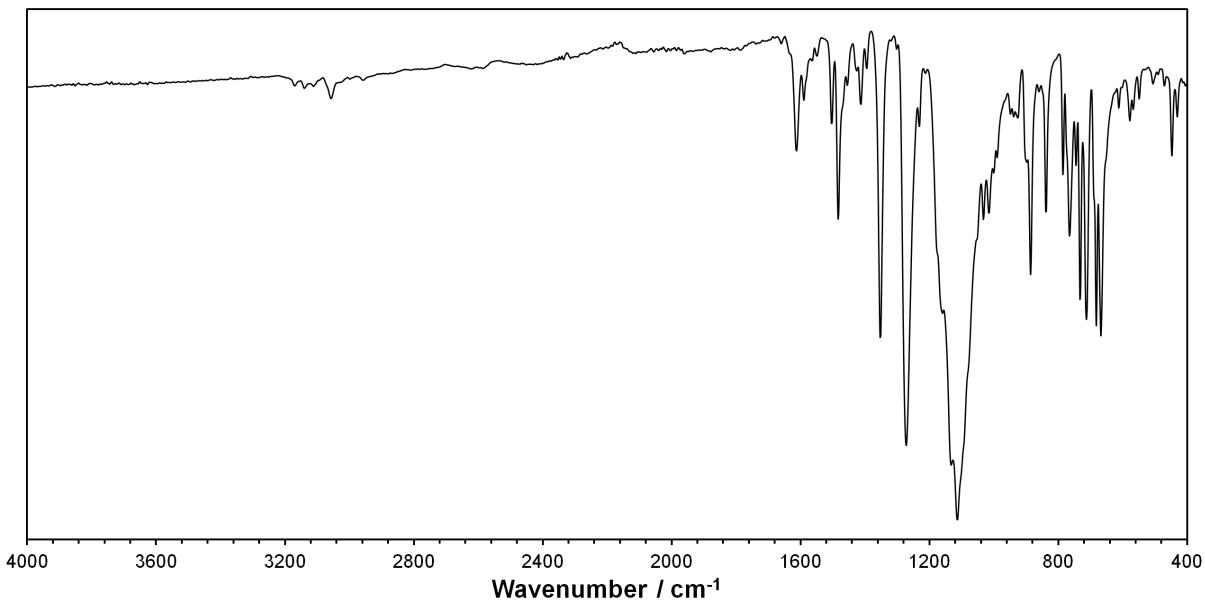

Figure S23. ATR IR spectrum of **1c**.

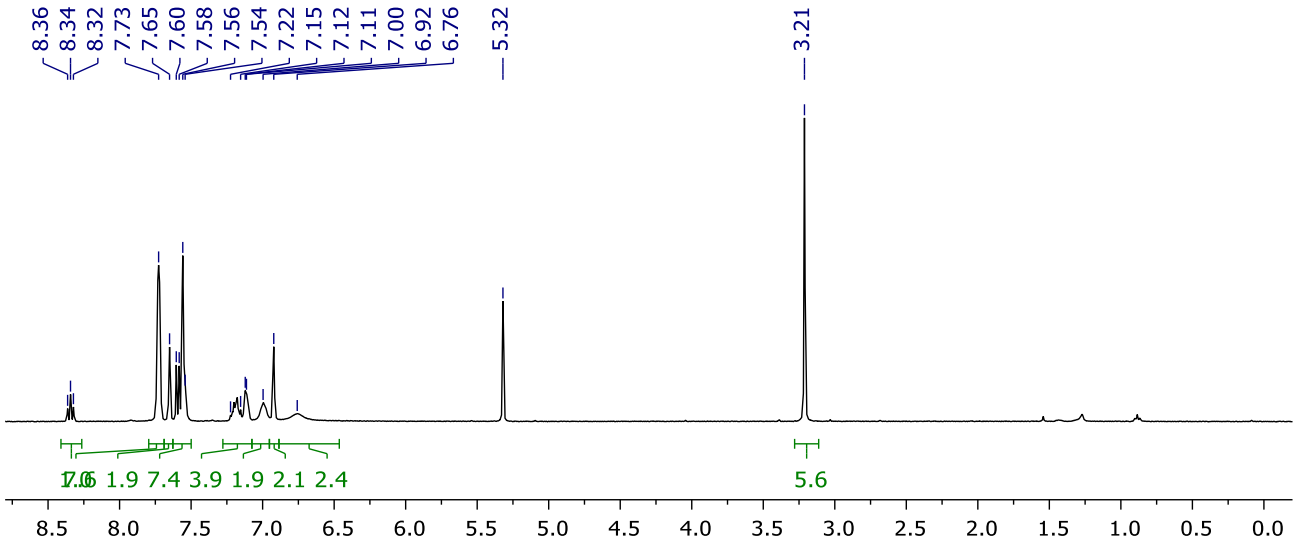

Figure S24. ^{1}H NMR spectrum recorded after **1c** was dissolved in CD_2Cl_2 (400 MHz).

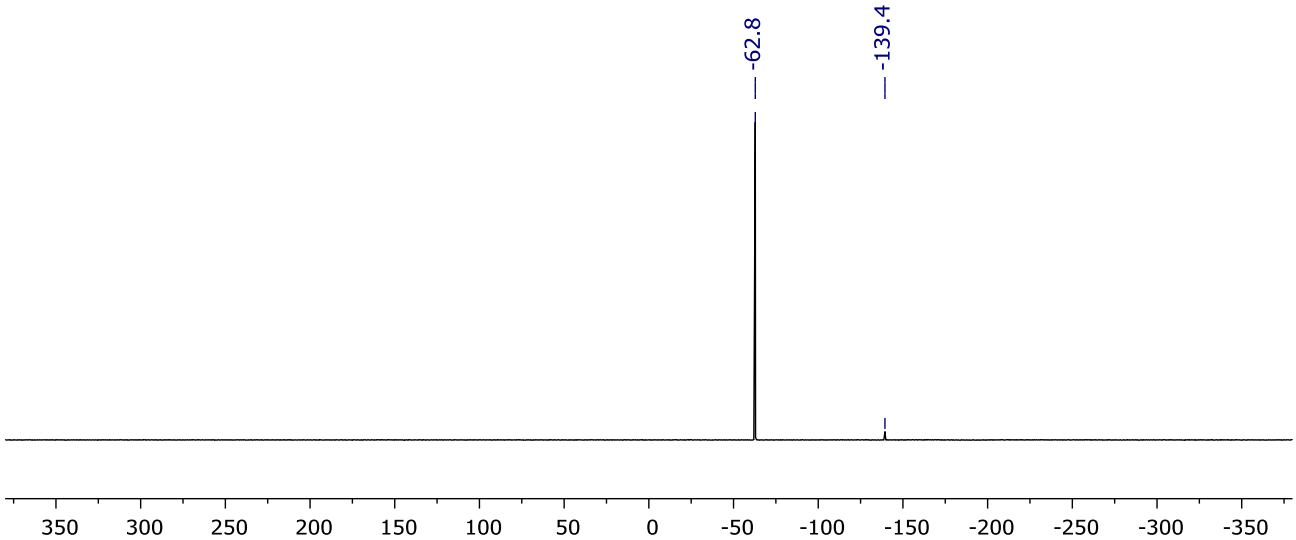

Figure S25. ^{19}F{^{1}H} NMR spectrum recorded after **1c** was dissolved in CD_2Cl_2 (377 MHz).

5.4 Arene = 1,3-$F_2C_6H_4$ (1d)

Following the general procedure using **2** (40.0 mg, 27.7 μmol) and 1,3-$F_2C_6H_4$ afforded **1d**. Yield: 31.2 mg (77%).

No absorbances attributed to bound fluoroarene could be detected on analysis by ATR IR spectroscopy. Analysis of a sample dissolved in CD_2Cl_2 by ^1H and ^{19}F NMR spectroscopy indicated the liberation of one equivalent of 1,3-$F_2C_6H_4$ into solution (δ_{19F} -110.8).

Anal. Calcd. for $C_{63}H_{37}BF_{26}N_5Rh$ (1471.70 gmol^{-1}): C, 51.42; H, 2.53; N, 4.76. Found C, 51.35; H, 2.38; N, 4.61.

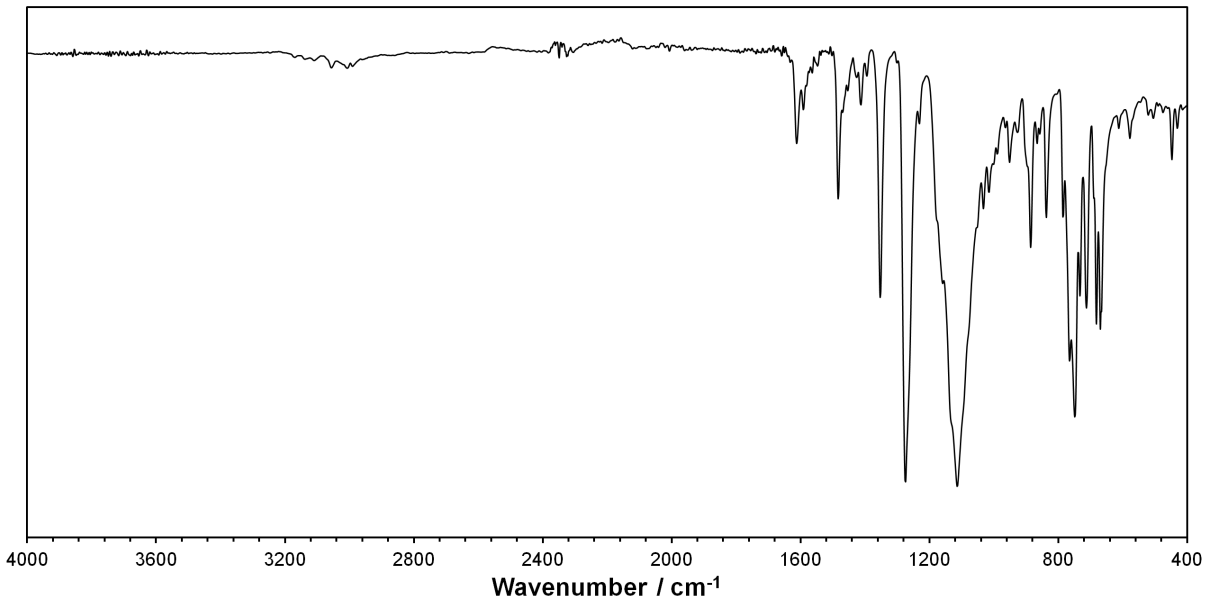

Figure S26. ATR IR spectrum of **1d**.

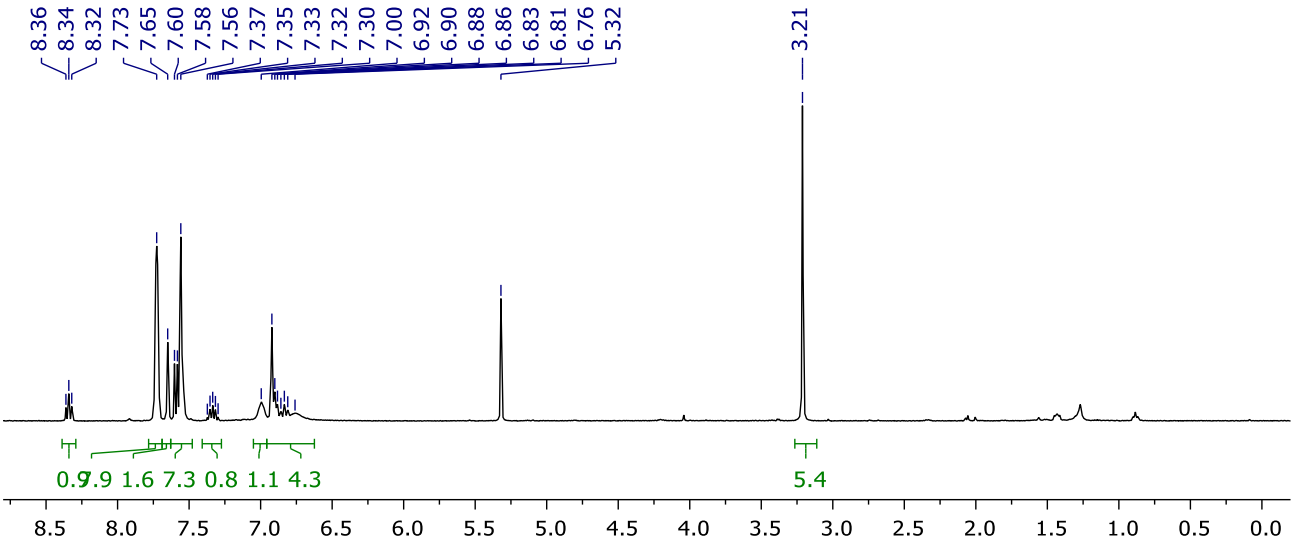

Figure S27 ^1H NMR spectrum recorded after **1d** was dissolved in CD_2Cl_2 (400 MHz).

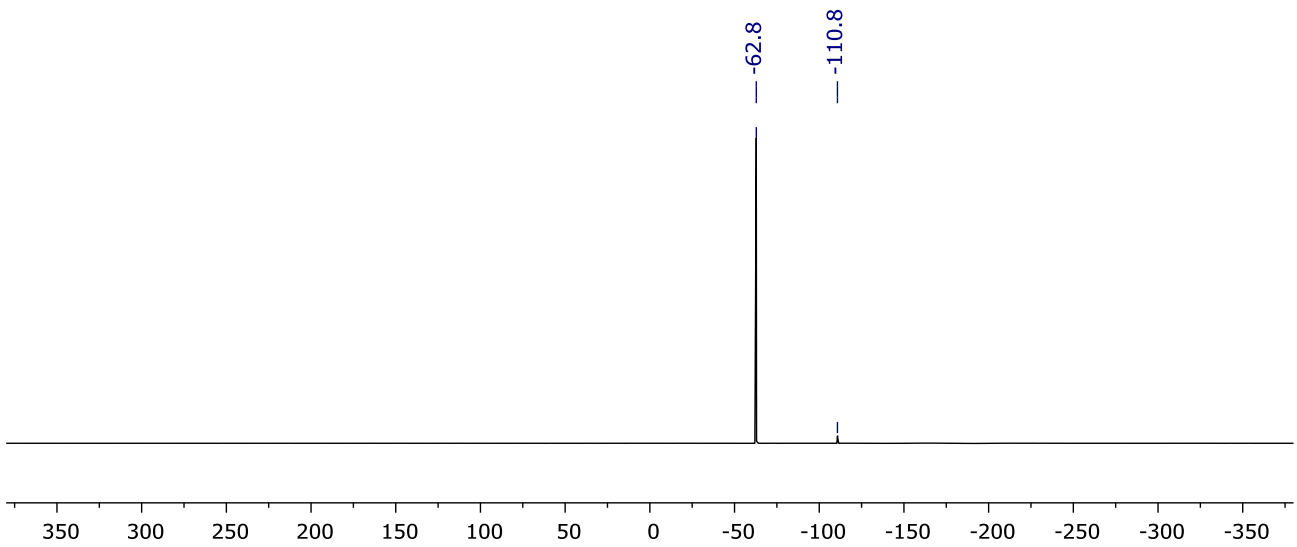

Figure S28. $^{19}F\{^{1}H\}$ NMR spectrum recorded after **1d** was dissolved in CD_2Cl_2 (377 MHz).

5.5 Arene = 1,4-$F_2C_6H_4$ (1e)

Following the general procedure using **2** (40.0 mg, 27.7 µmol) and 1,4-$F_2C_6H_4$ afforded **1e**. Yield: 32.9 mg (81%).

No absorbances attributed to bound fluoroarene could be detected on analysis by ATR IR spectroscopy. Analysis of a sample dissolved in CD_2Cl_2 by ^{1}H and ^{19}F NMR spectroscopy indicated the liberation of one equivalent of 1,4-$F_2C_6H_4$ into solution (δ_{19F} -120.3).

Anal. Calcd. for $C_{63}H_{37}BF_{26}N_5Rh$ (1471.70 gmol^{-1}): C, 51.42; H, 2.53; N, 4.76. Found C, 51.25; H, 2.32; N, 4.54.

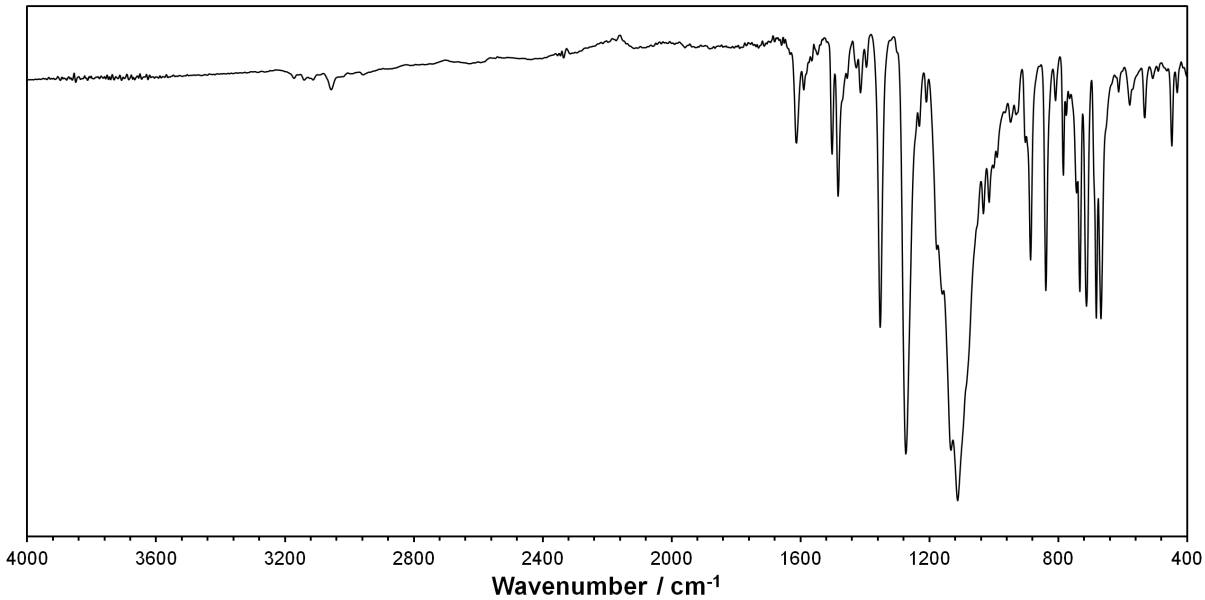

Figure S29. ATR IR spectrum of **1e**.

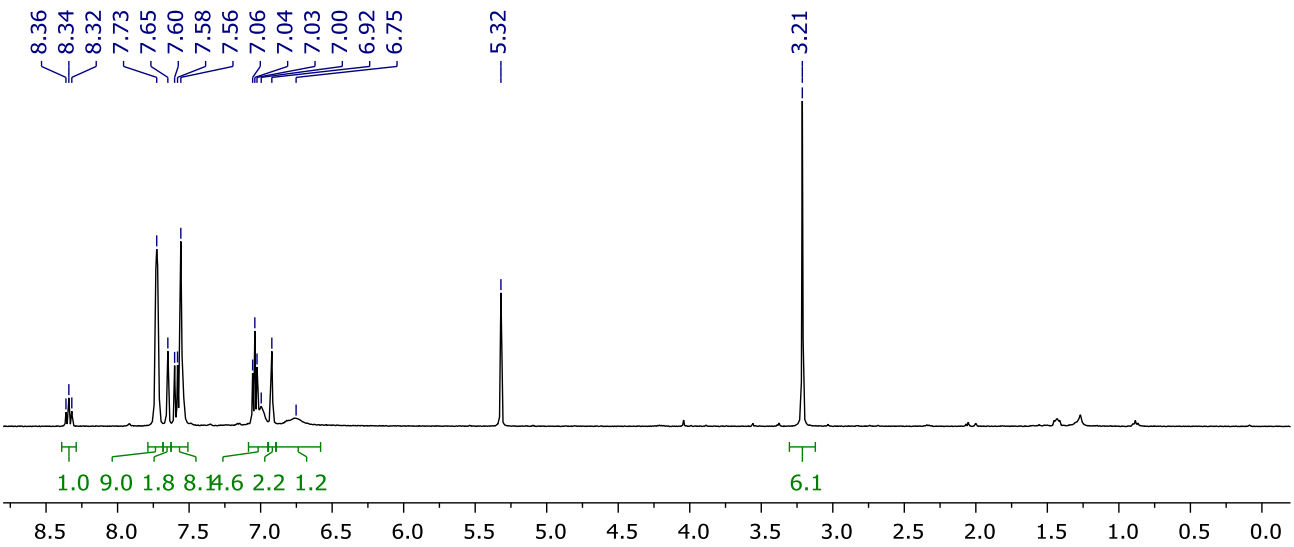

Figure S30. ^{1}H NMR spectrum recorded after **1e** was dissolved in CD_2Cl_2 (400 MHz).

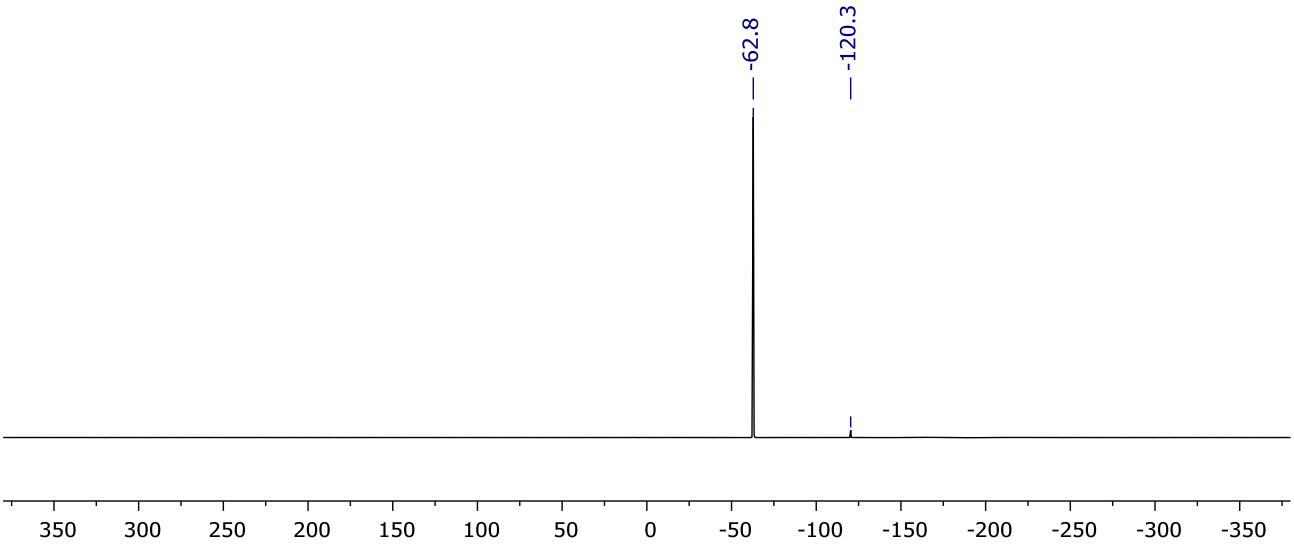

Figure S31. ^{19}F{^{1}H} NMR spectrum recorded after **1e** was dissolved in CD_2Cl_2 (377 MHz).

5.6 Competition experiment and preparation of 1a

A solution of **2** (40.0 mg, 27.7 µmol) in 1,2-$F_2C_6H_4$ (*ca.* 2 mL) was briefly mixed before volatiles were removed *in vacuo*. The residue was dissolved in a mixture of 1,2-$F_2C_6H_4$ (1.00 mL, 10.2 mmol) and C_6H_6 (910 µL, 10.2 mmol) causing a colour change from orange to yellow. After 30 min the solution was layered with excess hexane (*ca.* 50 mL) and stored at RT to afford **1a** as yellow-orange crystals. Yield: 30.7 mg (77%).

No signals attributed to bound arene could be detected on analysis by ATR IR spectroscopy. Analysis of a sample dissolved in CD_2Cl_2 by ^{1}H and ^{19}F NMR spectroscopy confirmed the absence of fluoroarene and liberation of one equivalent of C_6H_6 into solution.

Anal. Calcd. for $C_{63}H_{37}BF_{26}N_5Rh$ (1471.70 gmol^{-1}): C, 51.42; H, 2.53; N, 4.76. Found C, 51.25; H, 2.32; N, 4.54.

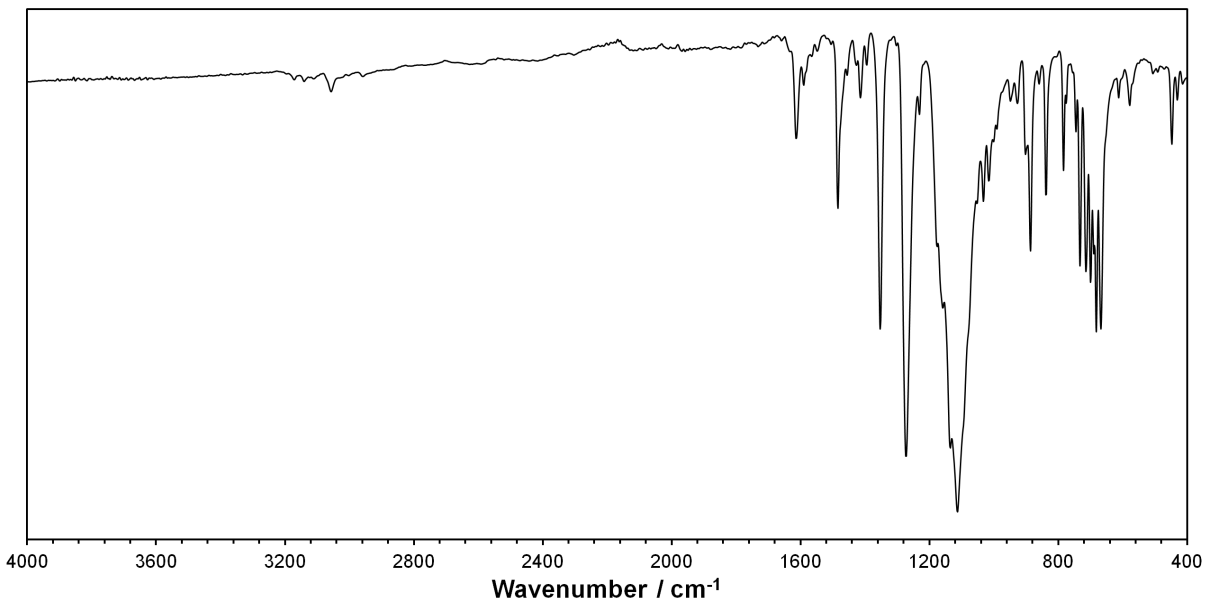

Figure S32. ATR IR spectrum of **1a**.

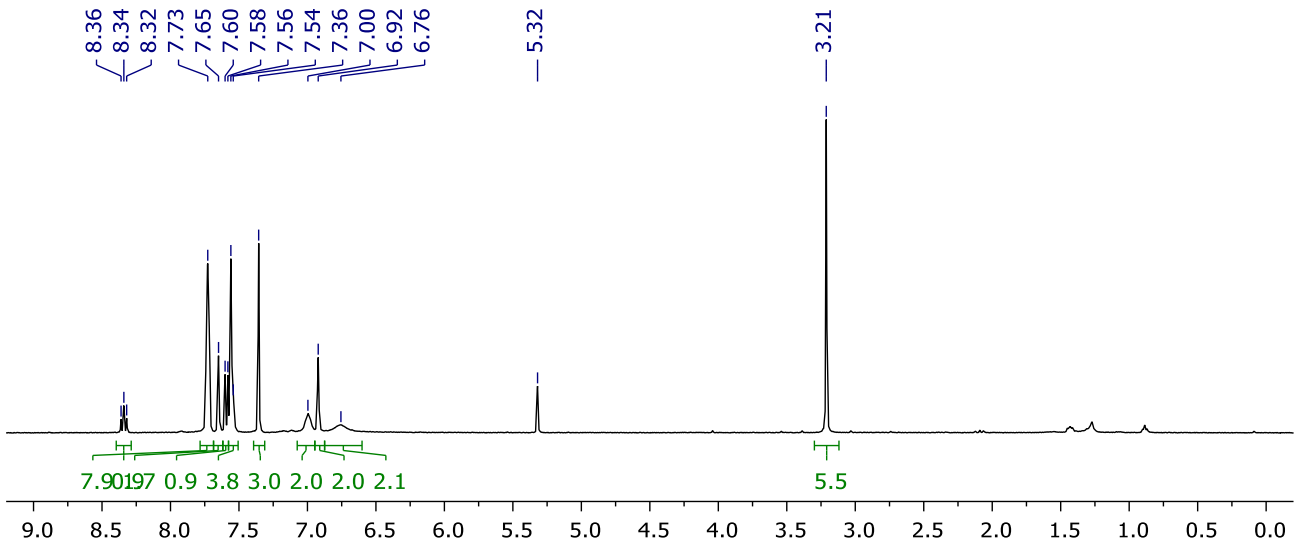

Figure S33. ^{1}H NMR spectrum recorded after **1a** was dissolved in CD_2Cl_2 (400 MHz).

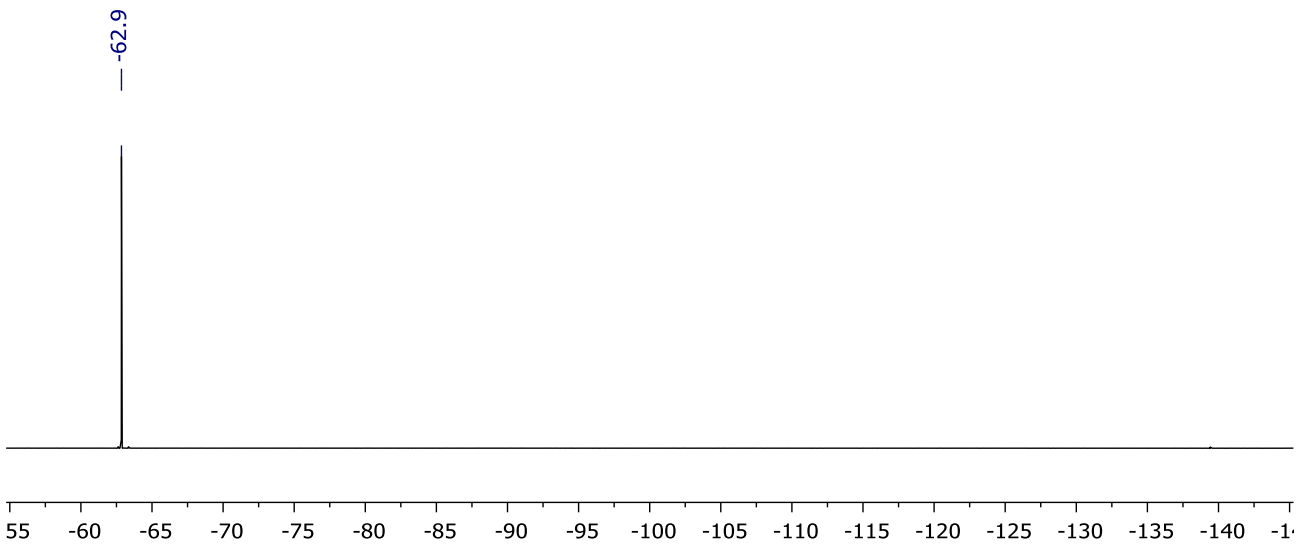

Figure S34. ^{19}F{^{1}H} NMR spectrum recorded after **1a** was dissolved in CD_2Cl_2 (377 MHz).

5.7 Analysis by SS ^{19}F MAS NMR spectroscopy

All solid-state NMR experiments were recorded on a Bruker 500 WB (wide bore) spectrometer equipped with AVANCE III console and using a 1.3 mm Bruker probe in HCN configuration at 50 kHz MAS frequency. The probe was tuned to ^{19}F frequency at 470.38 MHz and sample were maintained at 288 K with active cooling using a Bruker BCU-X cooling unit (670 L/h flow). The hard 90° pulses were set to 2.5 µs at 100 kHz nutation frequency for ^{19}F. The experiments were acquired with a single 2 s recycle delay and 256 scans were collected.

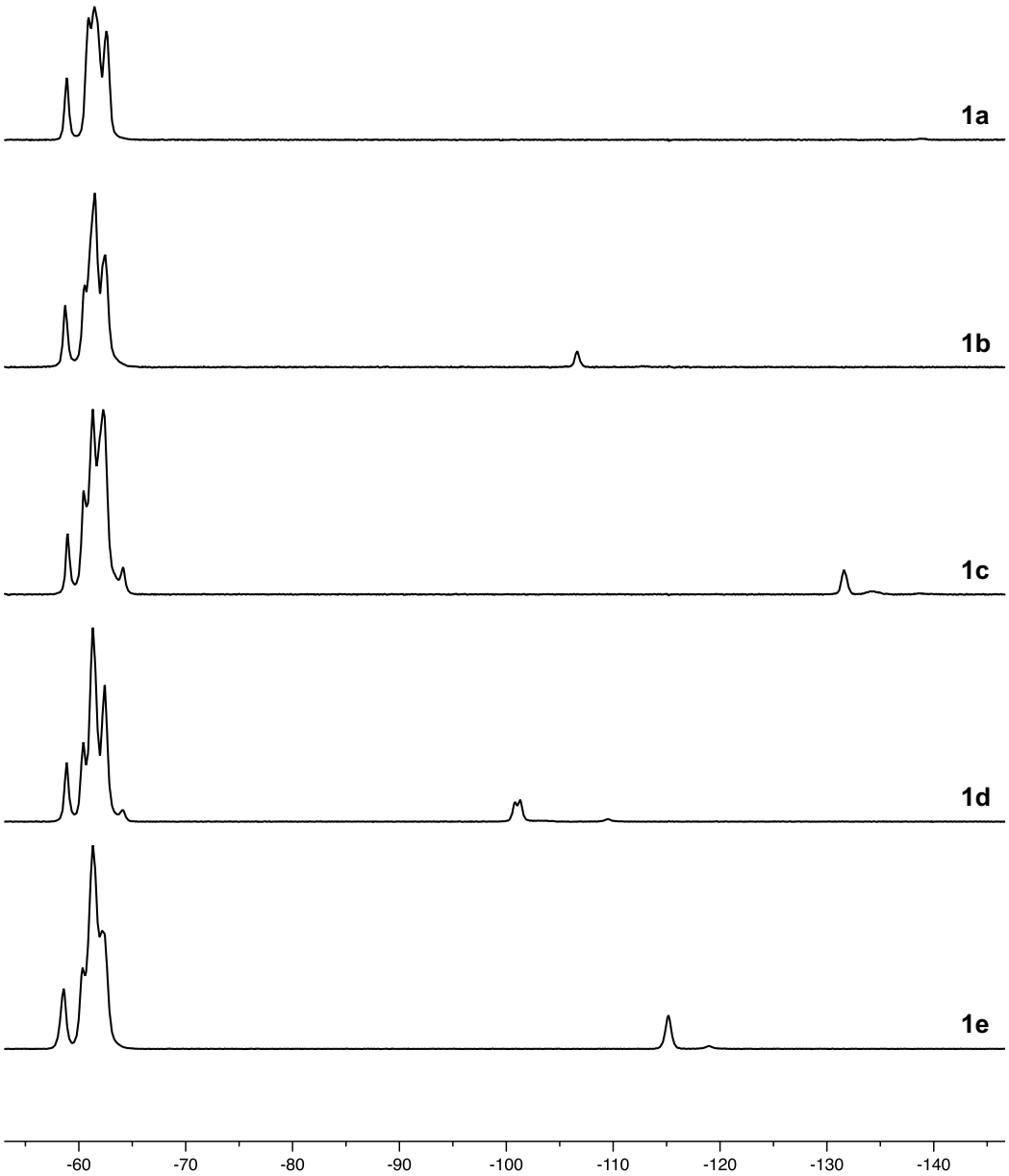

Figure S35. SS ^{19}F MAS NMR spectra of **1a–e** (470 MHz, 288 K).

6. Computational details

Density functional theory calculations were carried out using the ORCA 4.1.2 program,[4] employing Grimme's dispersion corrected ωB97X-D3 functional[5] and the def2-TZVP(-f) basis set on all atoms, with the associated def2-ECP effective core potential on Rh and Re.[6] The RIJCOSX approximation was used to reduce the computational cost of calculations (with the def2/J auxiliary basis set).[7] Geometries of metal cations were optimised starting from the X-ray crystallography data and are provided in XYZ format. Characterisation of stationary points as minima was verified by analytical vibrational mode analysis. Coordination of the fluoroarene moieties was investigated using the extended transition state method for energy decomposition analysis combined with the natural orbitals for chemical valence theory (ETS-NOCV) as implemented in ORCA 4.1.2.[8]

Table S2. Calculated binding energies and NOCV orbital stabilisation energies for the {Rh(CNC-Me)(biph)}$^+$/arene fragmentation (kJ mol^{-1}).

Compd_binding site	*E*	ΔE_{bind}	NOCV 1 (arene→M)	NOCV 2 (M→arene)	NOCV 1+2	NOCV total
1a	-1581.83769205	-73.8	-31.6	-6.8	-38.4	-56.6
1b_1,2	-1681.09138313	-63.8	-21.2	-2.8	-24.0	-40.2
1b_2,3	-1681.09464906	-72.4	-30.2	-7.2	-37.3	-56.4
1b_3,4	-1681.09383741	-70.2	-28.6	-6.0	-34.6	-52.8
1c_1,2	-1780.33691113	-51.8	-9.1	-1.9	-11.0	-23.3
1c_2,3	-1780.34048612	-61.2	-18.4	-3.1	-21.5	-38.3
1c_3,4	-1780.34344070	-69.0	-26.6	-6.2	-32.9	-52.3
1c_4,5	-1780.34294412	-67.7	-27.1	-5.7	-32.8	-51.6
1d_1,2	-1780.34759673	-63.0	-21.1	-3.1	-24.2	-41.0
1d_3,4	-1780.34695140	-61.3	-20.9	-2.7	-23.6	-40.2
1d_4,5	-1780.34989114	-69.0	-28.3	-6.5	-34.8	-53.9
1e_1,2	-1780.34534824	-60.2	-18.0	-2.5	-20.5	-37.0
1e_2,3	-1780.34917565	-70.3	-29.0	-7.9	-8.8	-57.2
Benzene	-232.25317265	-	-	-	-	-
FC_6H_5	-331.51066553	-	-	-	-	-
1,2-$F_2C_6H_4$	-430.76074338	-	-	-	-	-
1,3-$F_2C_6H_4$	-430.76717331	-	-	-	-	-
1,4-$F_2C_6H_4$	-430.76598094	-	-	-	-	-
[Rh(CNC-Me)(biph)]$^+$	-1349.55642465	-	-	-	-	-

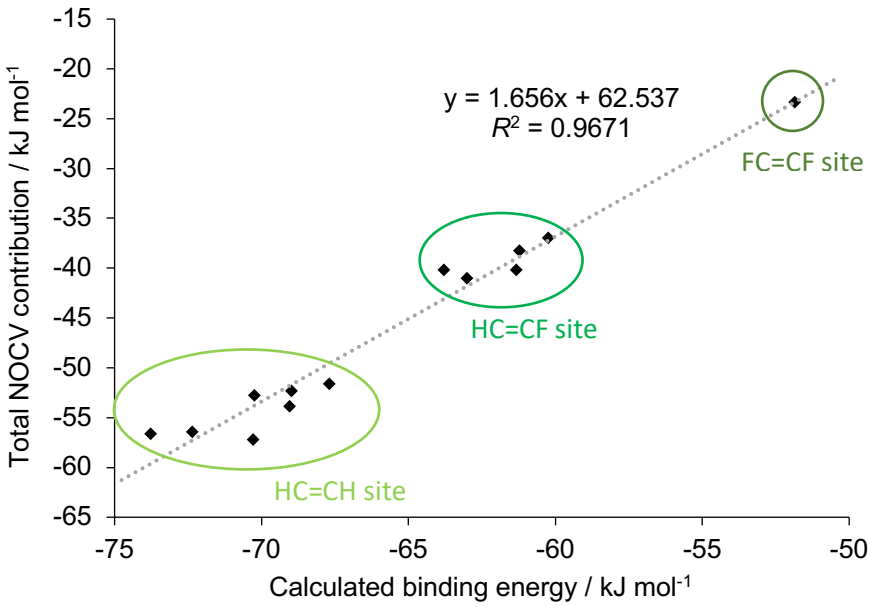

Figure S36. Plot showing the correlation between binding energy and total NOCV orbital stabilisation energy.

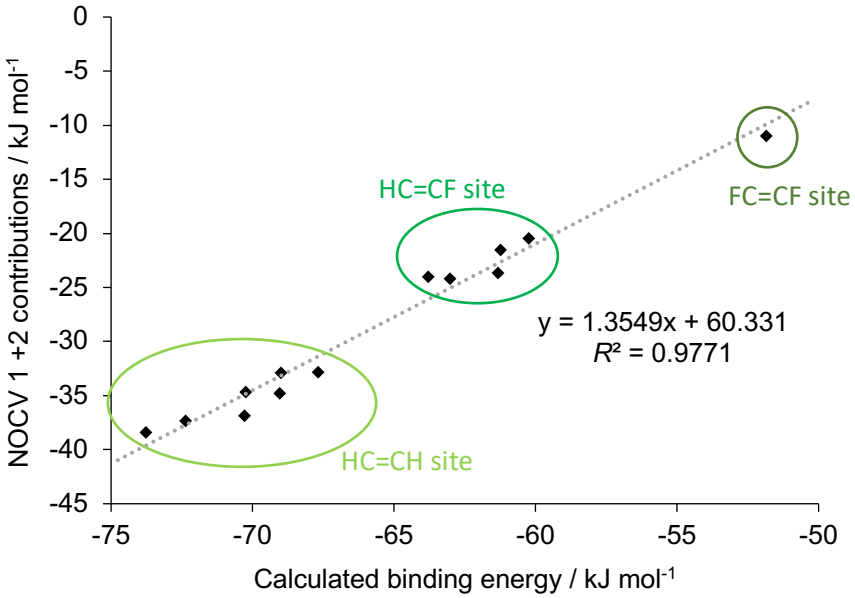

Figure S37. Plot showing the correlation plot binding energy and the sum of the NOCV 1 (arene→M) and NOCV 2 (M→arene) orbital stabilisation energies.

Table S3. Deformation densities associated with the {Rh(CNC-Me)(biph)}$^{+}$/arene fragmentation. Charge flow from red to blue.

Compd_binding site	NOCV 1 (arene→M)	NOCV 2 (M→arene)
1a	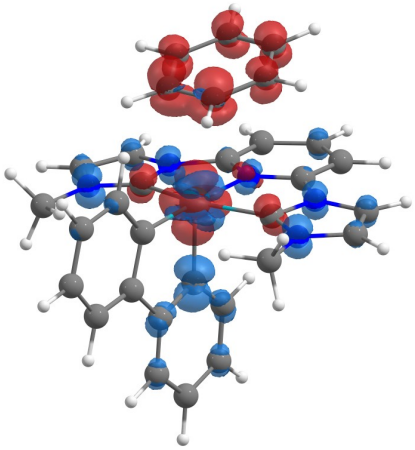	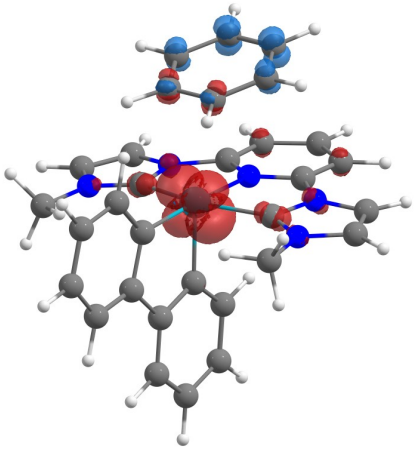
	$\Delta E_{\rho 1}$ = -31.6 kJ mol^{-1}	$\Delta E_{\rho 2}$ = -6.8 kJ mol^{-1}
	v_1 = 0.282	v_2 = 0.131
1b_1,2	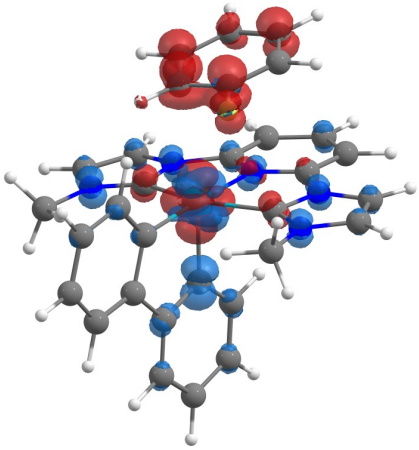	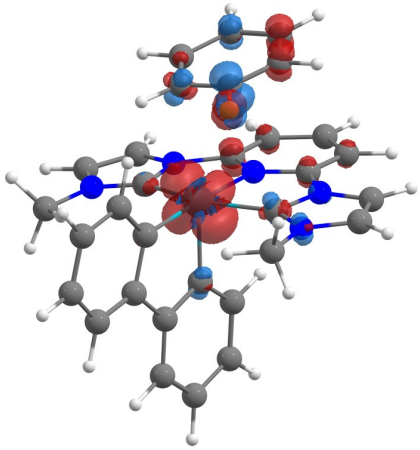
	$\Delta E_{\rho 1}$ = -21.2 kJ mol^{-1}	$\Delta E_{\rho 2}$ = -2.8 kJ mol^{-1}
	v_1 = 0.232	v_2 = 0.077
1b_2,3	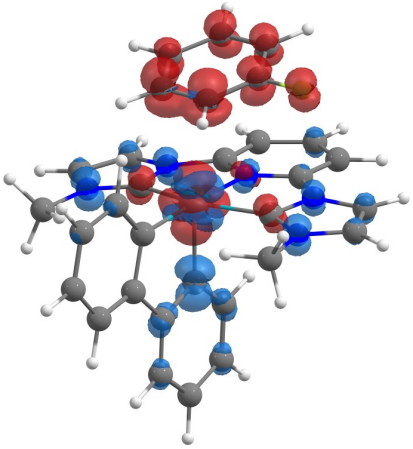	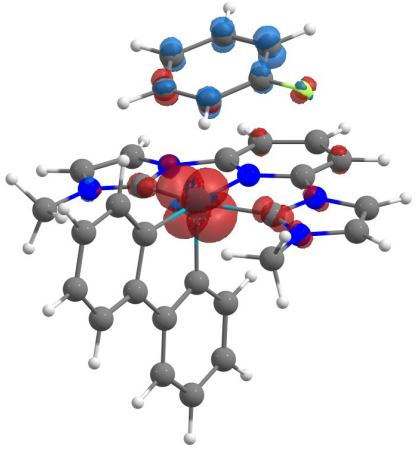
	$\Delta E_{\rho 1}$ = -30.2 kJ mol^{-1}	$\Delta E_{\rho 2}$ = -7.2 kJ mol^{-1}
	v_1 = 0.270	v_2 = 0.137

1b_3,4

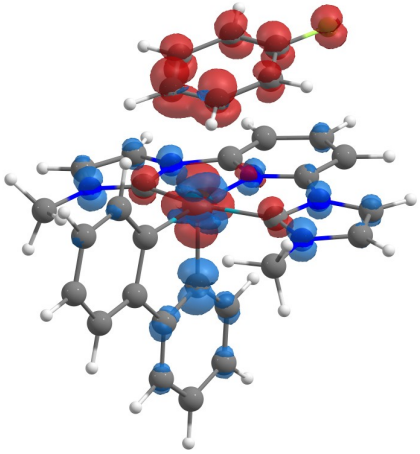

$\Delta E_{\rho 1}$ = -28.6 kJ mol^{-1}

v_1 = 0.268

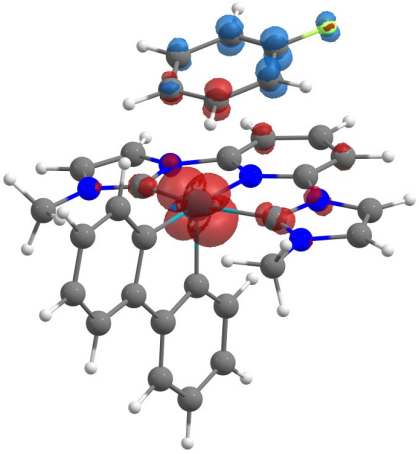

$\Delta E_{\rho 2}$ = -6.0 kJ mol^{-1}

v_2 = 0.124

1c_1,2

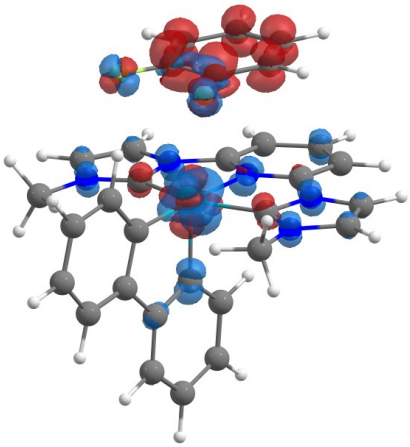

$\Delta E_{\rho 1}$ = -9.1 kJ mol^{-1}

v_1 = 0.149

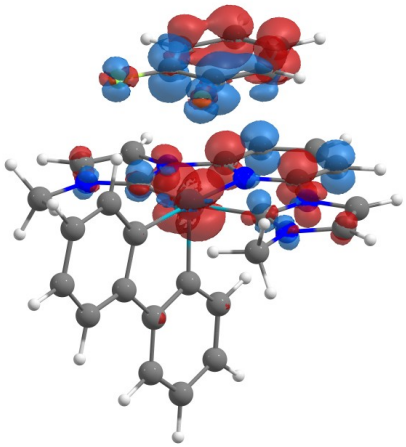

$\Delta E_{\rho 2}$ = -1.9 kJ mol^{-1}

v_2 = 0.056

1c_2,3

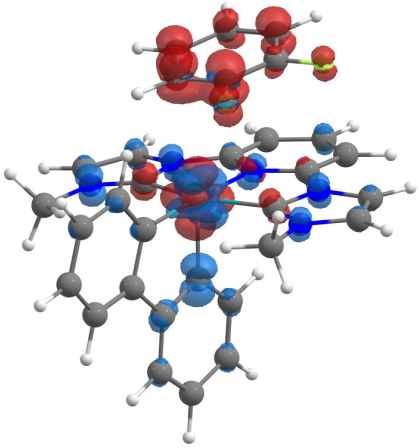

$\Delta E_{\rho 1}$ = -18.4 kJ mol^{-1}

v_1 = 0.213

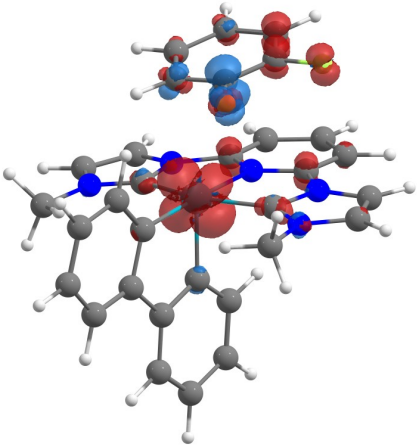

$\Delta E_{\rho 2}$ = -3.1 kJ mol^{-1}

v_2 = 0.083

1c_3,4

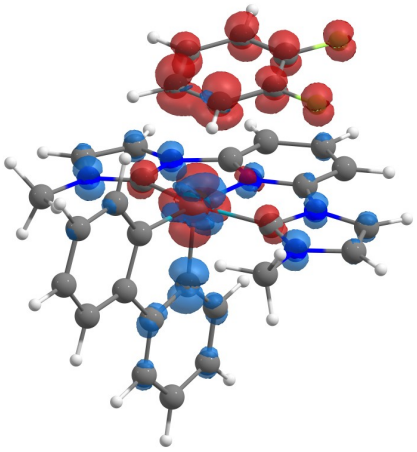

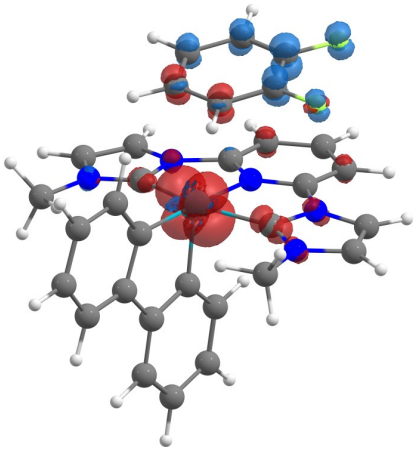

$\Delta E_{\rho 1}$ = -26.6 kJ mol^{-1}

v_1 = 0.253

$\Delta E_{\rho 2}$ = -6.2 kJ mol^{-1}

v_2 = 0.128

1c_4,5

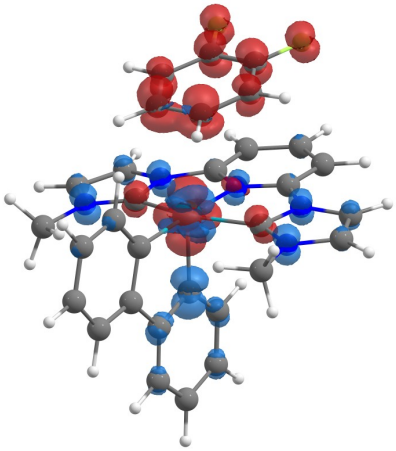

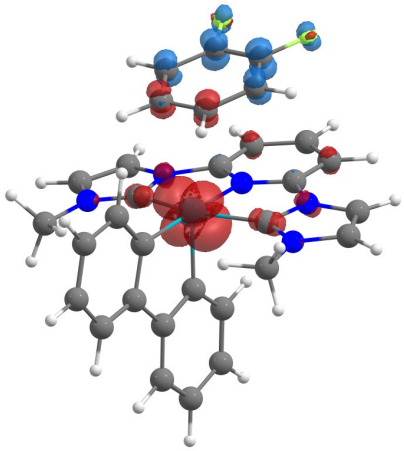

$\Delta E_{\rho 1}$ = -27.1 kJ mol^{-1}

v_1 = 0.260

$\Delta E_{\rho 2}$ = -5.7 kJ mol^{-1}

v_2 = 0.121

1d_1,2

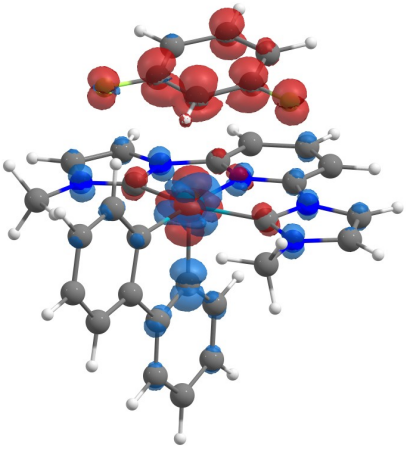

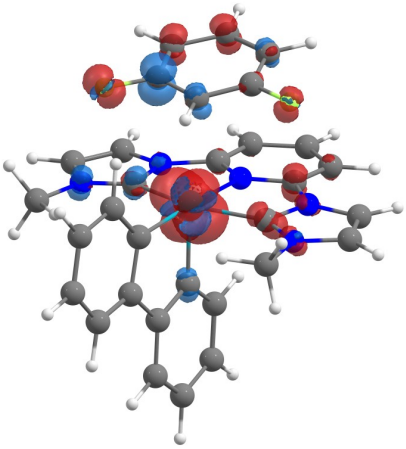

$\Delta E_{\rho 1}$ = -21.1 kJ mol^{-1}

v_1 = 0.225

$\Delta E_{\rho 2}$ = -3.1 kJ mol^{-1}

v_2 = 0.083

1d_3,4

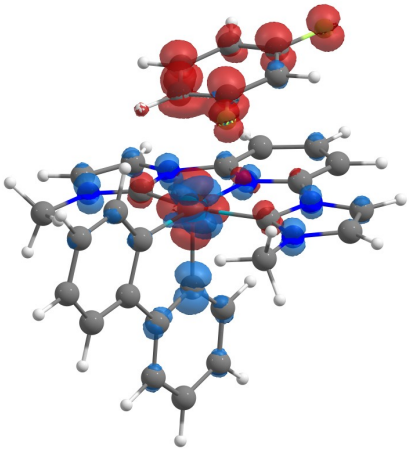

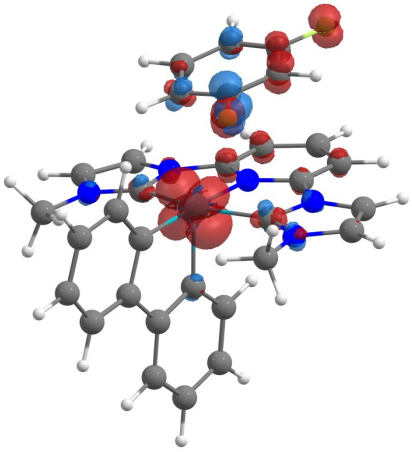

$\Delta E_{\rho 1}$ = -20.9 kJ mol^{-1}

v_1 = 0.231

$\Delta E_{\rho 2}$ = -2.7 kJ mol^{-1}

v_2 = 0.076

1d_4,5

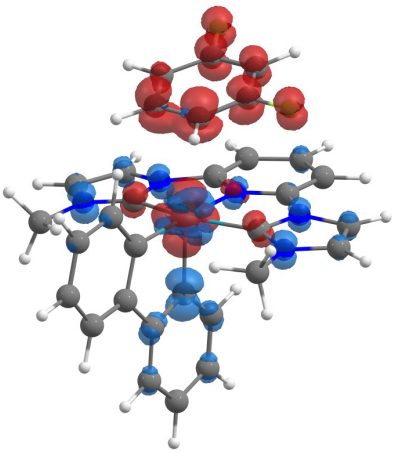

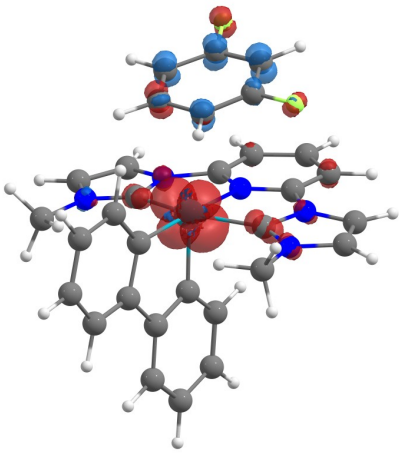

$\Delta E_{\rho 1}$ = -28.3 kJ mol^{-1}

v_1 = 0.261

$\Delta E_{\rho 2}$ = -6.5 kJ mol^{-1}

v_2 = 0.130

1e_1,2

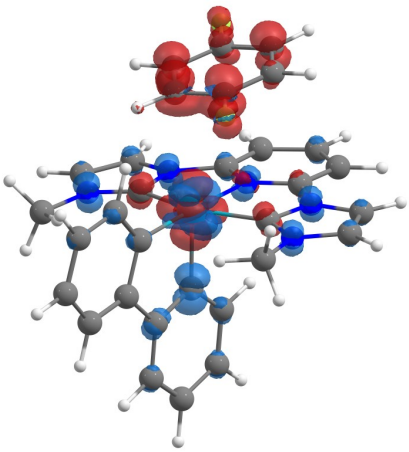

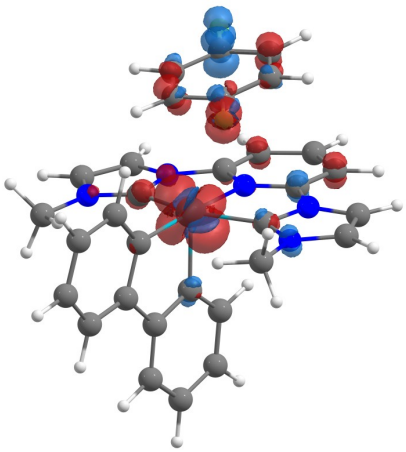

$\Delta E_{\rho 1}$ = -18.0 kJ mol^{-1}

v_1 = 0.211

$\Delta E_{\rho 2}$ = -2.5 kJ mol^{-1}

v_2 = 0.074

1e_2,3	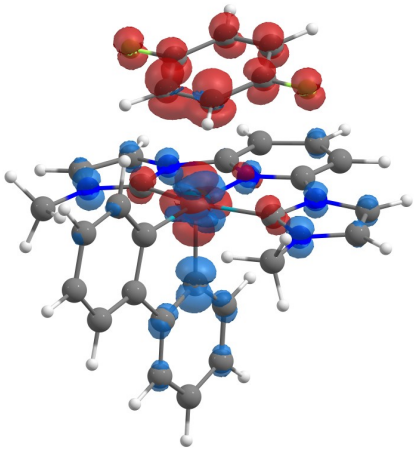	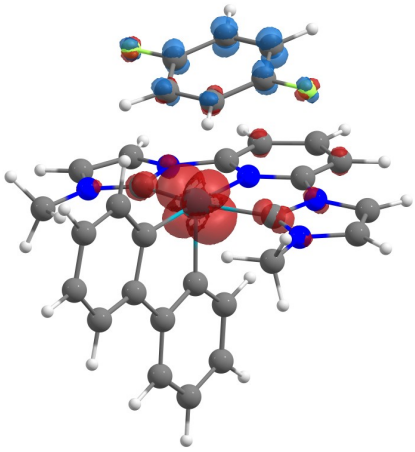
	$\Delta E_{\rho 1}$ = -29.0 kJ mol^{-1}	$\Delta E_{\rho 2}$ = -7.9 kJ mol^{-1}
	v_1 = 0.259	v_2 = 0.147

7. References

[1] W. E. Buschmann, J. S. Miller, K. Bowman-James and C. N. Miller, *Inorg. Synth.*, 2002, **33**, 83–91.

[2] D. S. McGuinness, J. A. Suttil, M. G. Gardiner and N. W Davies, *Organometallics*, 2008, **27**, 4238–4247.

[3] C. N. Iverson and W. D. Jones, *Organometallics*, 2001, **20**, 5745–5750.

[4] F. Neese, *Wiley Interdiscip. Rev. Comput. Mol. Sci.* 2018, **8**, e1327; F. Neese, *Wiley Interdiscip. Rev. Comput. Mol. Sci.* 2012, **2**, 73–78;

[5] Y.-S. Lin, G.-D. Li, S.-P. Mao and J.-D. Chai, *J. Chem. Theory Comput.* 2013, **9**, 263–272; S. Grimme, J. Antony, S. Ehrlich and H. Krieg, *J. Chem. Phys.* 2010, **132**, 263–272.

[6] F. Weigend and R. Ahlrichs, *Phys. Chem. Chem. Phys.* 2005, **7**, 3297–3305; T. Leininger, A. Nicklass, W. Küchle, H. Stoll, M. Dolg and A. Bergner, *Chem. Phys. Lett.* 1996, **255**, 274–280.

[7] F. Neese, F. Wennmohs, A. Hansen and U. Becker, *Chem. Phys.* 2009, **356**, 98–109; F. Weigend, *Phys. Chem. Chem. Phys.* 2006, **8**, 1057–1065.

[8] A. Altun, F. Neese and G. Bistoni, *J. Chem. Theory Comput.* 2019, **15**, 215–228; M. P. Mitoraj, A. Michalak and T. Ziegler, *J. Chem. Theory Comput.* 2009, **5**, 962–975.